SUPPORTING INFORMATION

Synthesis and chemical recycling of biobased poly(acetal-ester)s with a non-cyclic acetal unit

Niklas Warlin,[a,b] Sathiyaraj Subramaniyan,[a] Maria Nelly Garcia Gonzalez,[c] Rafael N. L.de Menezes,[a] Smita V. Mankar,[a,d] Nitin Valsange,[a] Nicola Rehnberg,[a,e] Patric Jannasch*[a] and Baozhong Zhang*[a]

[a] Centre of Analysis and Synthesis, Department of Chemistry, Lund University, P.O. Box 124, SE-22100 Lund, Sweden.

[b] Department of Chemistry, Stanford University, Stanford, California 94305-5080, United States

[c] Environmental and Energy Systems Studies, Department of Technology and Society, Lund University, PO Box 118, SE-221 00 Lund, Sweden

[d] Department of Chemical Engineering, Massachusetts Institute of Technology, 77 Massachusetts Avenue, Cambridge, Massachusetts 02139, United States.

[e] Bona Sweden AB, R&D, Box 210 74, SE-200 21 Malmö, Sweden.

1. NMR spectra of Monomers 1 and 2

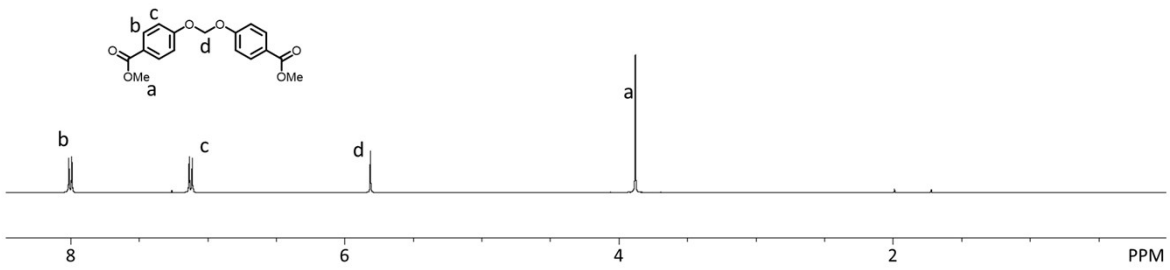

Figure S1. ^{1}H NMR spectrum of **1**.

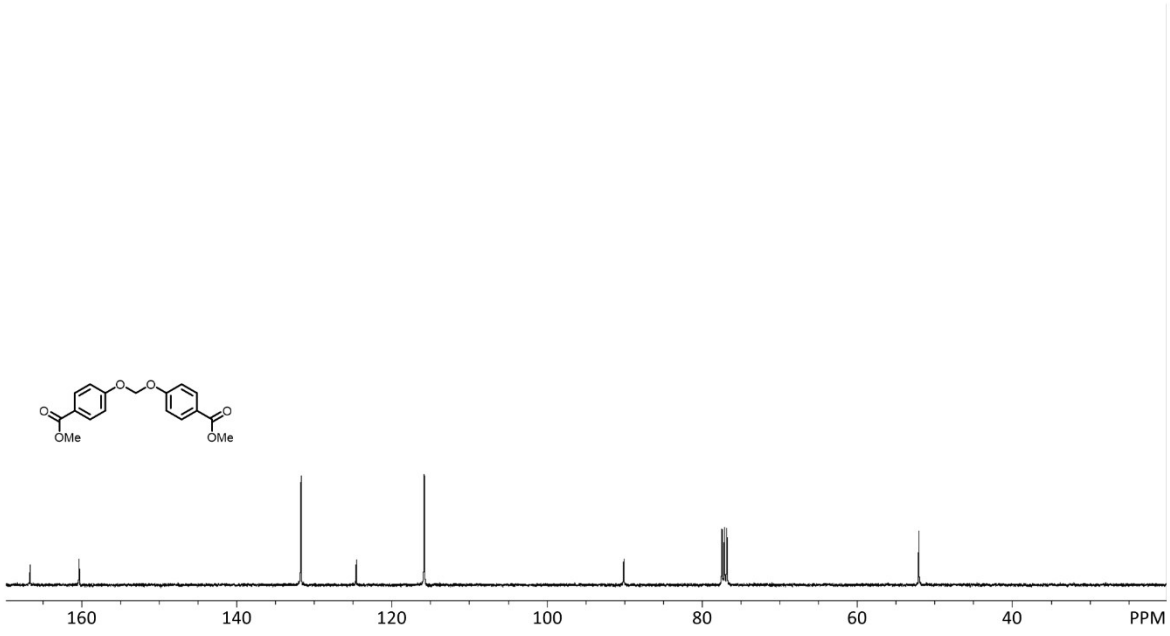

Figure S2. ^{13}C NMR spectrum of **1**.

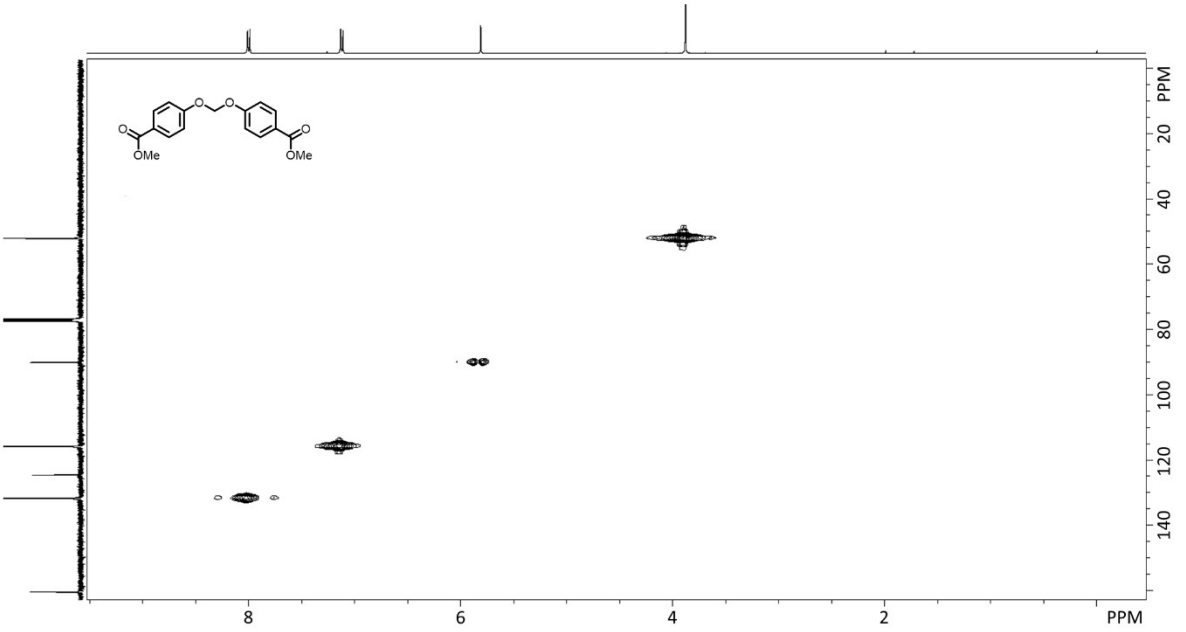

Figure S3. HMQC spectrum of **1**.

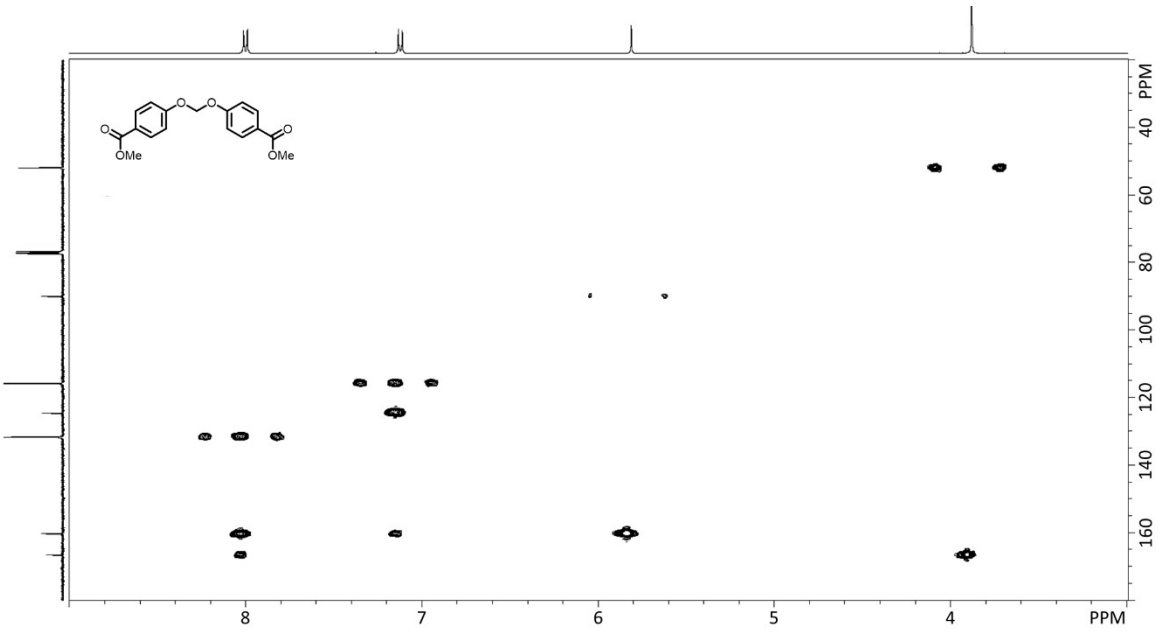

Figure S4. HMBC spectrum of **1**.

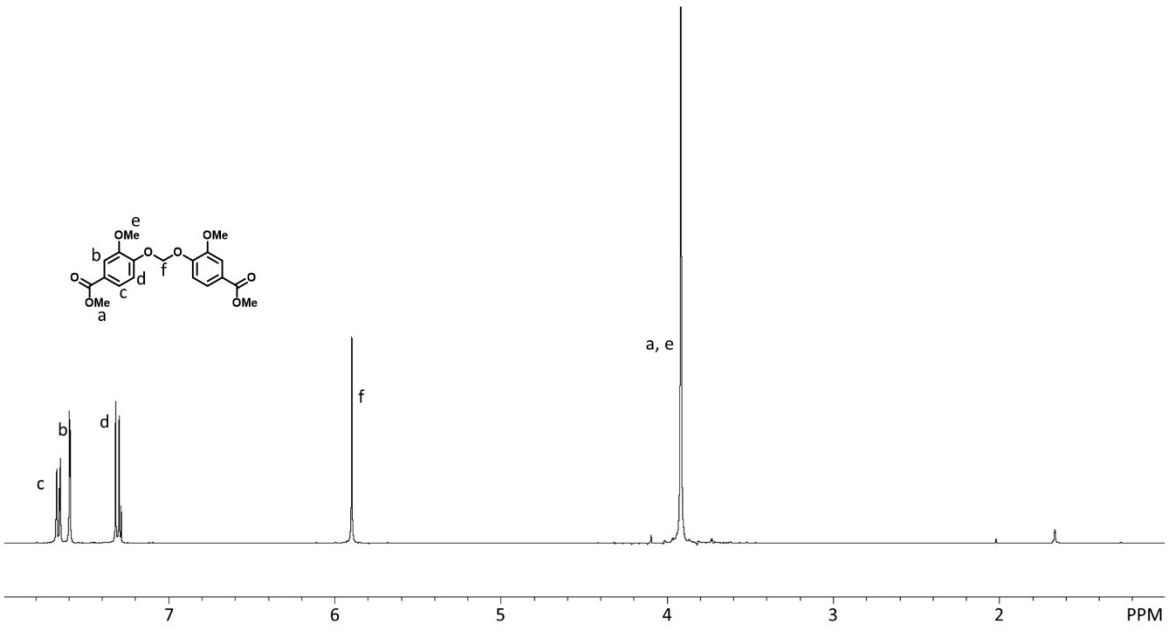

Figure S5. ^{1}H NMR spectrum of **2**.

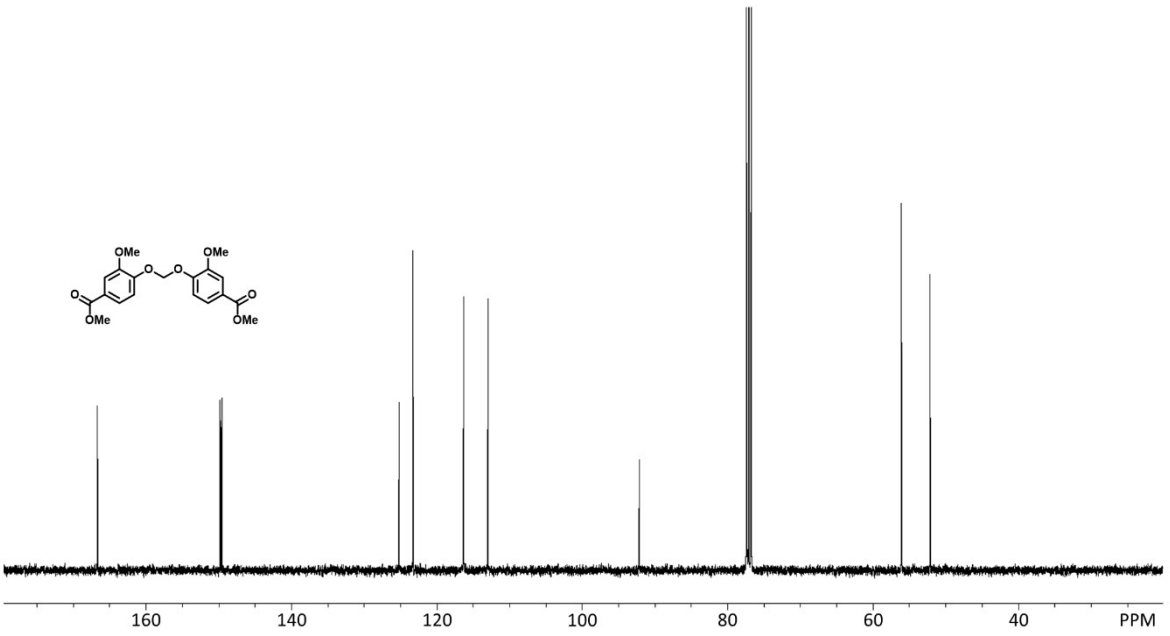

Figure S6. ^{13}C NMR spectrum of **2**.

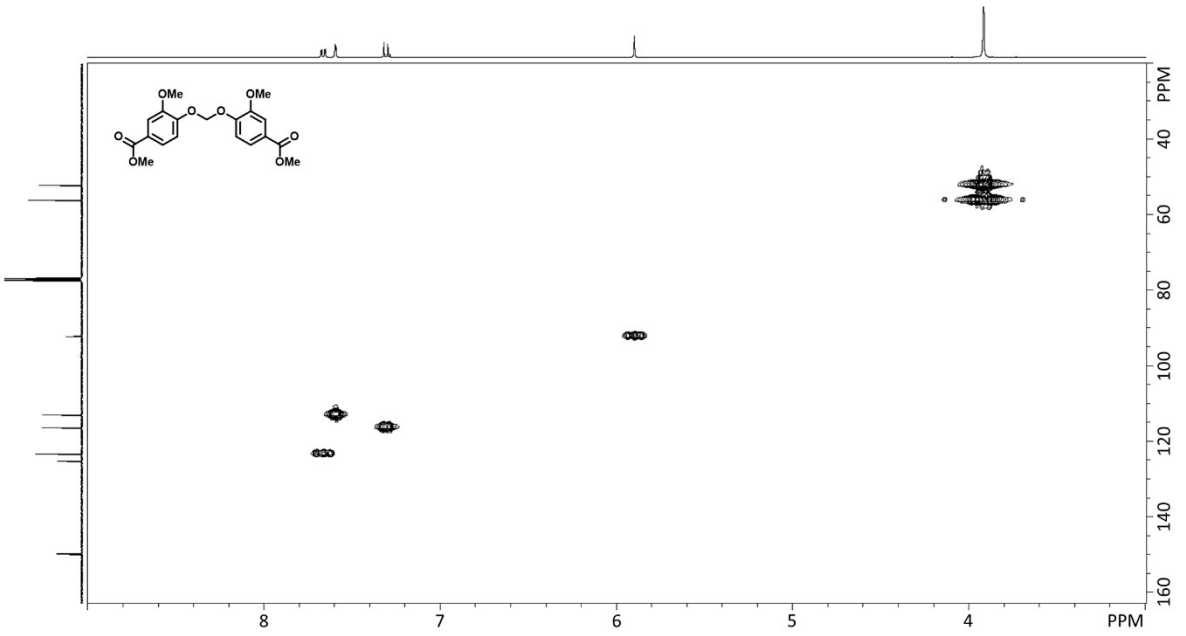

Figure S7. HMQC spectrum of **2**.

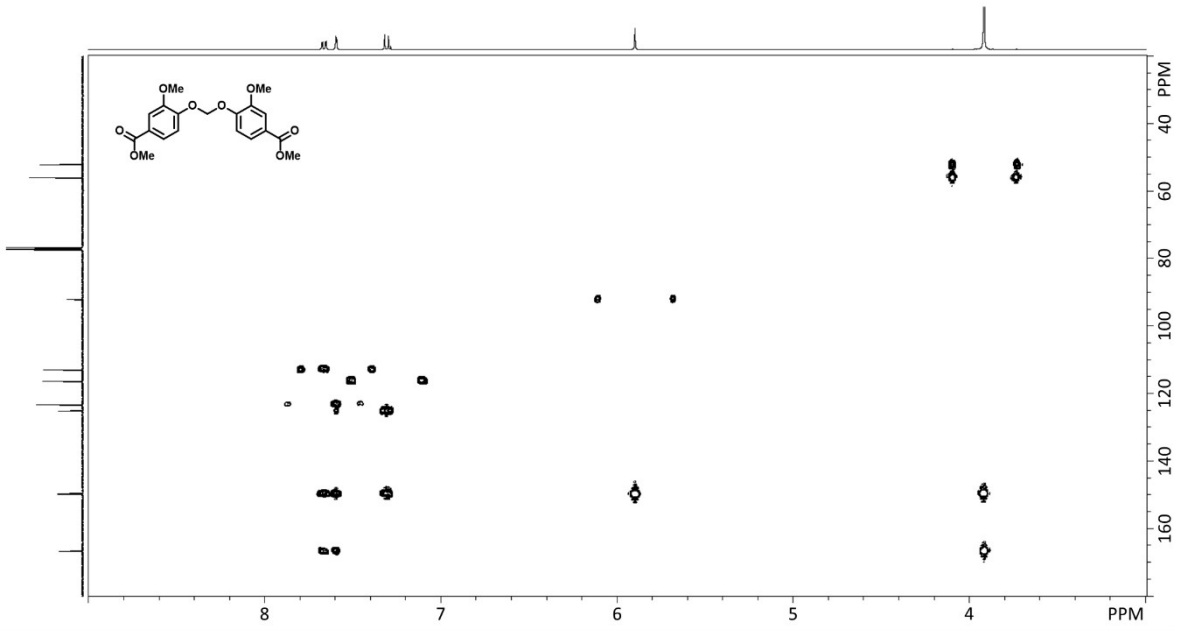

Figure S8. HMBC spectrum of **2**.

2. LCA of Monomers 1 and 2

The energy required to heat the reaction was calculated according to Eq. 1.

$$q_{heating} = q_{PVC} * \frac{T_{reaction} - T_{RT}}{T_{PVC} - T_{RT}}$$

Eq. 1

where $q_{heating}$ is the energy required to heat the reaction to the reaction temperature, q_{PVC} is the energy used for heating during emulsion polymerization of PVC (taken from the SimaPro software), $T_{reaction}$ is the reaction temperature, T_{RT} is room temperature (which was estimated to 20 °C), and T_{PVC} is the reaction temperature used for emulsion polymerisation of PVC (which was estimatd to 80 °C).

Table S1. Summary of the cradle-to-gate LCA of monomer 1 and 2, and the 3 largest contributions in terms of GHG emissions.

Monomer	**Total GHG emissions (kg CO_2 eq/kg monomer)**	**Largest contribution (kg CO_2 eq/kg monomer)**	**2nd largest contribution (kg CO_2 eq/kg monomer)**	**3rd largest contribution (kg CO_2 eq/kg monomer)**
1	12.4	7.16 (*p* - HBA production)	3.61 (K_2CO_3 production)	1.15 (DCM production)
2	5.45	2.89 (K_2CO_3 production)	1.11 (Van acid production)	0.92 (DCM production)

Table S2. Three reaction parameters (i.e., base, temperature, solvent) were optimized toward high conversion and low climate impact for the synthesis of Monomer **1**. The parameters and the results were color coded to illustrate sustainability, with green being the most sustainable, yellow the intermediately sustainable, and red the least sustainable.

	Parameters			Results	
Reaction	**Base[a]**	**Temperature[b] (°C)**	**Solvent[c]**	**Conversion[d] (%)**	**Climate Impact[e] (kg CO_2 eq. / kg monomer)**
A*	K_2CO_3	82	ACN	**88**	12.4
B	K_2CO_3	56	Acetone	**82**	13.9
C	K_2CO_3	20	DMSO	50	22.3
D	K_2CO_3	20	Acetone	0	-
E	NaOH	82	ACN	**95**	**9.38**
F	NaOH	82	DMSO	**85**	**10.4**
G	NaOH	82	*t*-BuOH	58	15.1
H	NaOH	56	DMSO	**99**	**8.88**
I	NaOH	56	ACN	34	25.2
J	NaOH	56	*t*-BuOH	0	-
K	NaOH	20	DMSO	43	19.1
L	NaOH	30	*t*-BuOH	0	-
M	NaOH	20	Acetone	0	-

* The initial non-optimized reaction conditions for synthesis of monomer **1**. [a] Color-coded according to the GHG emissions of the production of the two bases. [b] Higher reaction temperatures were generally less favorable due to energy consumption. [c] Color-coded according to the CHEM21 solvent guide. [d] The conversion after 24 h according to ^{1}H NMR spectroscopy. High conversions (above 80%) were color-coded green, medium to low conversions (34-58%) were yellow, and non-conversion was red. [e] Climate impacts lower than the non-optimized reaction **A*** (i.e., < 12.4 kg CO_2 eq./kg) were color-coded green, higher climate impacts (i.e., 12.4-25.2 kg CO_2 eq./kg) were color-coded yellow, and climate impacts which could not be calculated (due to the low conversion) were color-coded red.

The GHG emissions in this work are expressed as Global Warming Potential (GWP), which is an index to measure how much infrared thermal radiation a greenhouse gas (GHG) would absorb over a given time frame. For the synthesis of Monomers **1** and **2**, GWP values were calculated as 12.4 and 5.5 kg CO_2 eq. / kg monomer (Table S1), respectively, according to the method described in the Experimental session. It is noteworthy that difference between the GWP results of monomers **1** and **2** mainly stems from their different starting materials, as the GWP for biobased vanillic acid from Borregaard was calculated from an industrial scale production while the only available GWP data for 4-HBA by Krömer et al was calculated for pilot-scale synthesis.[1,2] Additionally, the study conducted by Borregaard included the down-stream process. As such, the calculated results should be interpreted with caution, and a more comprehensive analysis is necessary before any final conclusion can be drawn. Subsequently,

three key reaction parameters that can affect the GHG emissions (the choice of base, reaction temperature, and solvent selection) were evaluated in the synthesis of Monomer **1** from an environmental impact perspective. The goal of this optimization was to maintain relatively high yields (i.e., >80%), while simultaneously lowering the GHG emissions. As shown in Entry A-D (Table S2), lowering the temperature when K_2CO_3 was used as the base was in general not preferred because it decreased the yield and increased the climate impact. The only case which was somewhat improved was condition **B**, which utilized a more environmentally benign solvent (i.e., acetone) at mild temperature while the results (i.e., the conversion and climate impact) were only slightly inferior to condition **A**, which used the more harmful solvent acetonitrile. Furthermore, a stronger base with low GHG emissions (i.e., NaOH) was investigated. Consequently (Table S2, conditions **E**–**G**), the reactions performed at high temperatures (82 °C) reached relatively high conversions and low GHG emissions. Particularly polar aprotic solvents such as ACN and DMSO were necessary to reach high conversions (95 % and 85 %, respectively) and low climate impacts (9.38 and 10.4 kg CO_2 eq./kg respectively). Interestingly, the polar protic solvent *t*-BuOH could only produce moderate conversion and climate impact (58 % and 15.1 kg CO_2 eq./kg respectively). This could be explained by the ability of polar aprotic solvents to activate nucleophiles in S_N2 reactions.[3] When the temperature was lowered to 56 °C, the conversion decreased significantly for both ACN and *t*-BuOH (Table 1, condition **I** and **J**), which could be explained by the reduced reaction rate at lower temperature. As a result, the estimated climate impact remained relatively high under these conditions. Interestingly, DMSO still produced high conversion and low climate impacts (99 % and 8.88 kg CO_2 eq./kg respectively) at this temperature, indicating that this could be the optimal condition if the temperature was a primal concern. Finally, the temperature was lowered to around room temperature (20-30 °C). In these cases, DMSO was the only solvent which could produce some conversion (Entry **K**), making these conditions less desirable.

3. GPC results for P1a-c and P2a-c

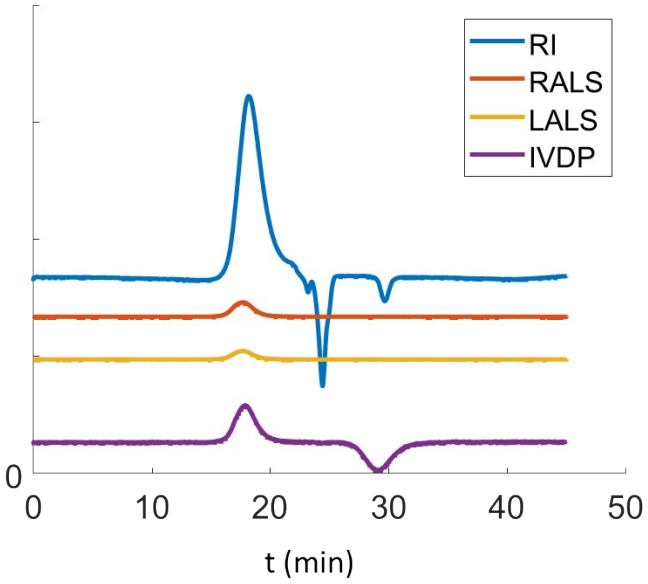

Figure S9. SEC curves of **P1a**, with signals from multi-detectors (RI: refractive index, RALS: right angle light scattering; LALS: low angle light scattering; IVDP: intrinsic viscosity-differential pressure).

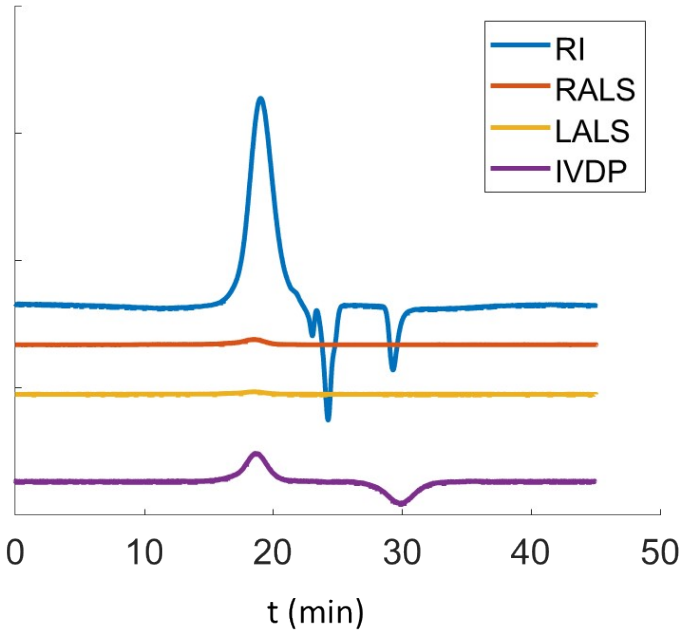

Figure S10. SEC curves of **P1b**, with signals from multi-detectors (RI: refractive index, RALS: right angle light scattering; LALS: low angle light scattering; IVDP: intrinsic viscosity-differential pressure).

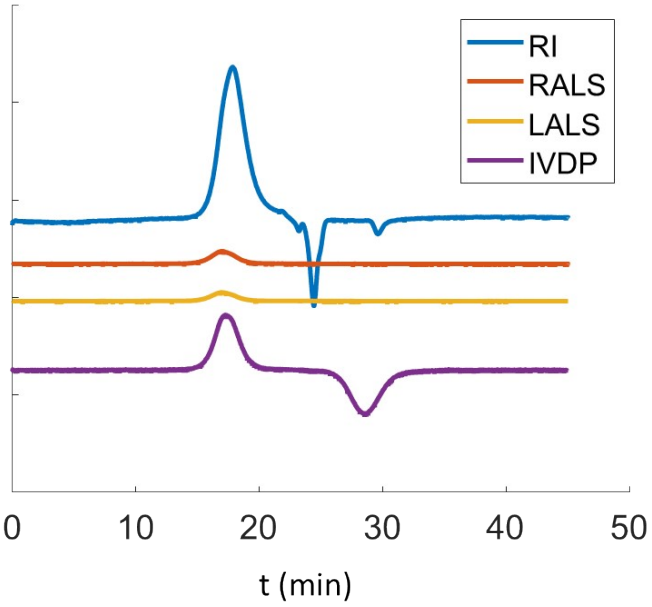

Figure S11. SEC curves of **P1c**, with signals from multi-detectors (RI: refractive index, RALS: right angle light scattering; LALS: low angle light scattering; IVDP: intrinsic viscosity-differential pressure).

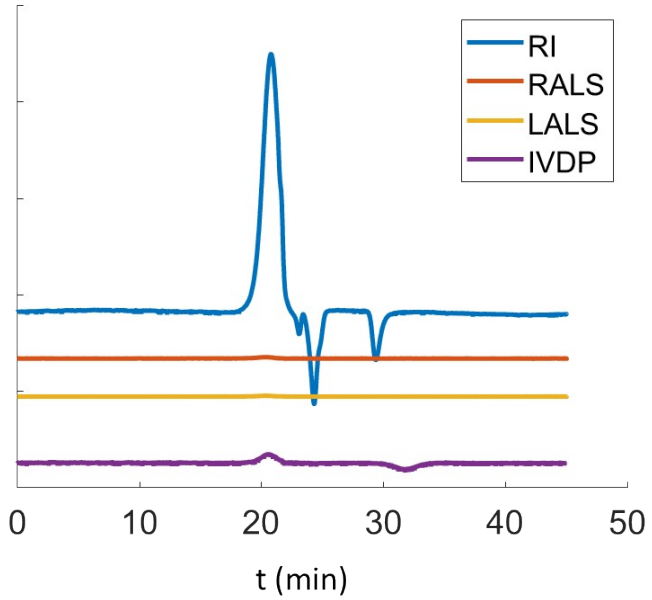

Figure S12. SEC curves of **P2a**, with signals from multi-detectors (RI: refractive index, RALS: right angle light scattering; LALS: low angle light scattering; IVDP: intrinsic viscosity-differential pressure).

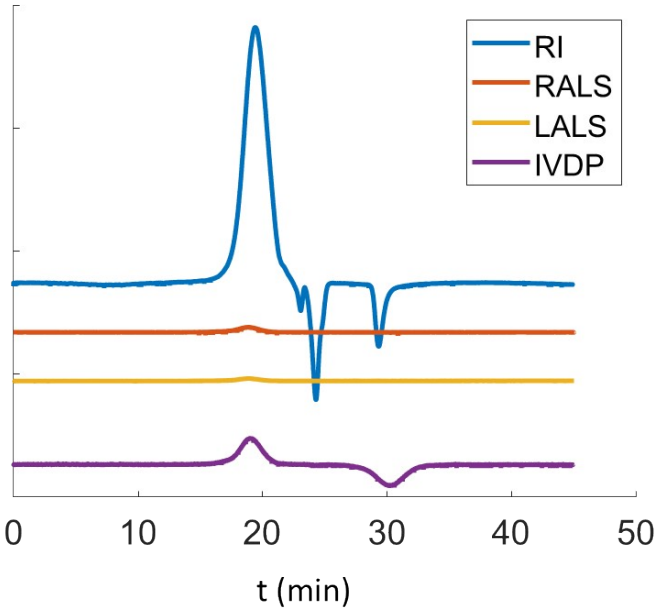

Figure S13. SEC curves of **P2b**, with signals from multi-detectors (RI: refractive index, RALS: right angle light scattering; LALS: low angle light scattering; IVDP: intrinsic viscosity-differential pressure).

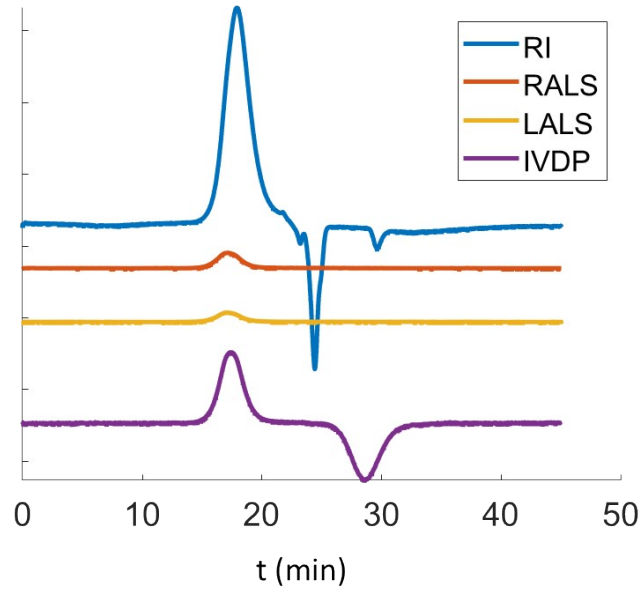

Figure S14. SEC curves of **P2c**, with signals from multi-detectors (RI: refractive index, RALS: right angle light scattering; LALS: low angle light scattering; IVDP: intrinsic viscosity-differential pressure).

4. NMR spectra for P1a-c and P2a-c

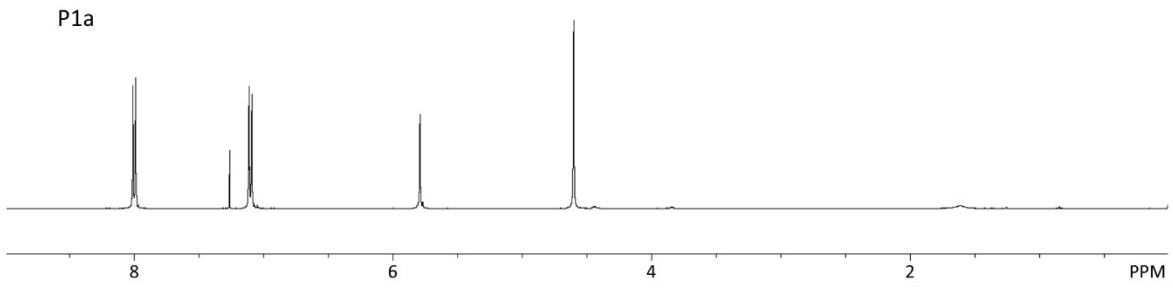

Figure S15. ^{1}H NMR spectrum of **P1a**.

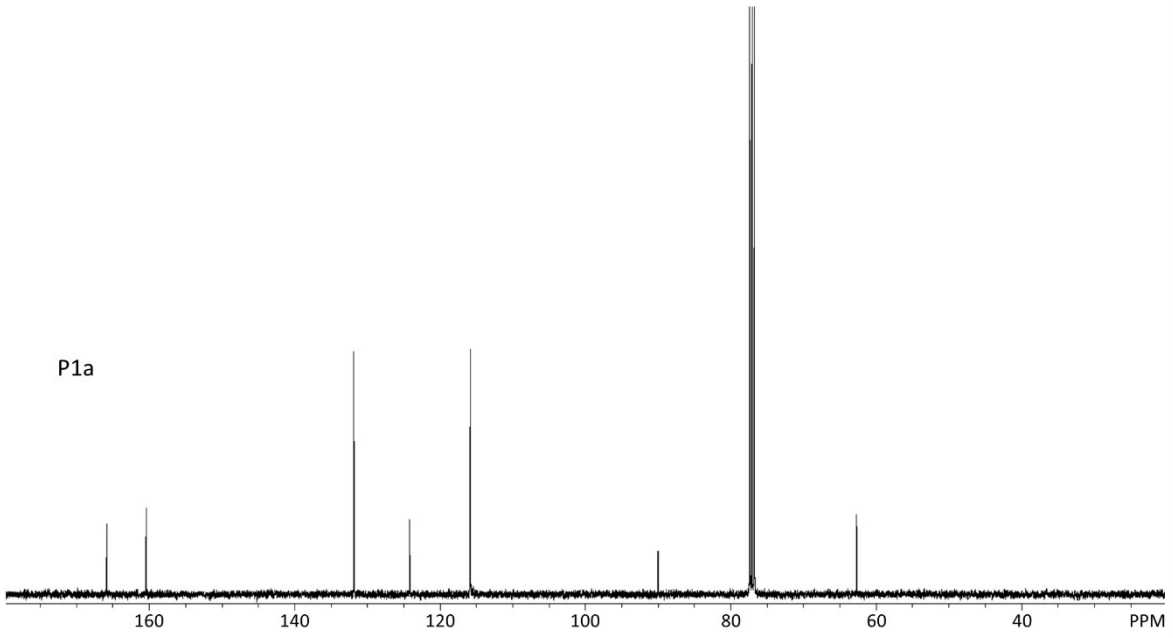

Figure S16. ^{13}C NMR spectrum of **P1a**.

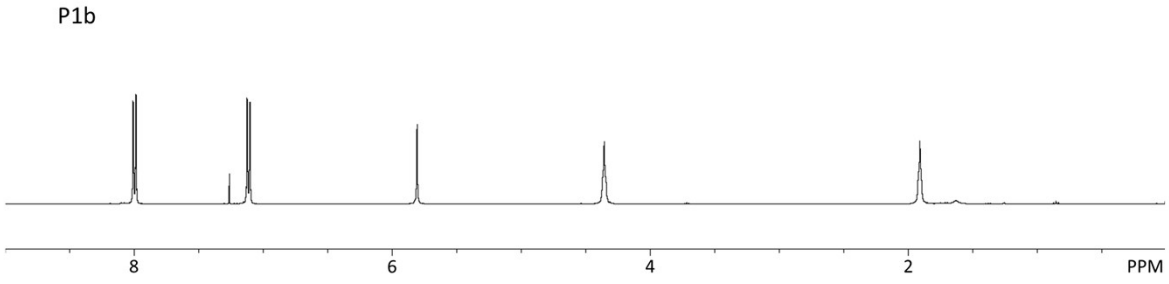

Figure S17. ^{1}H NMR spectrum of **P1b**.

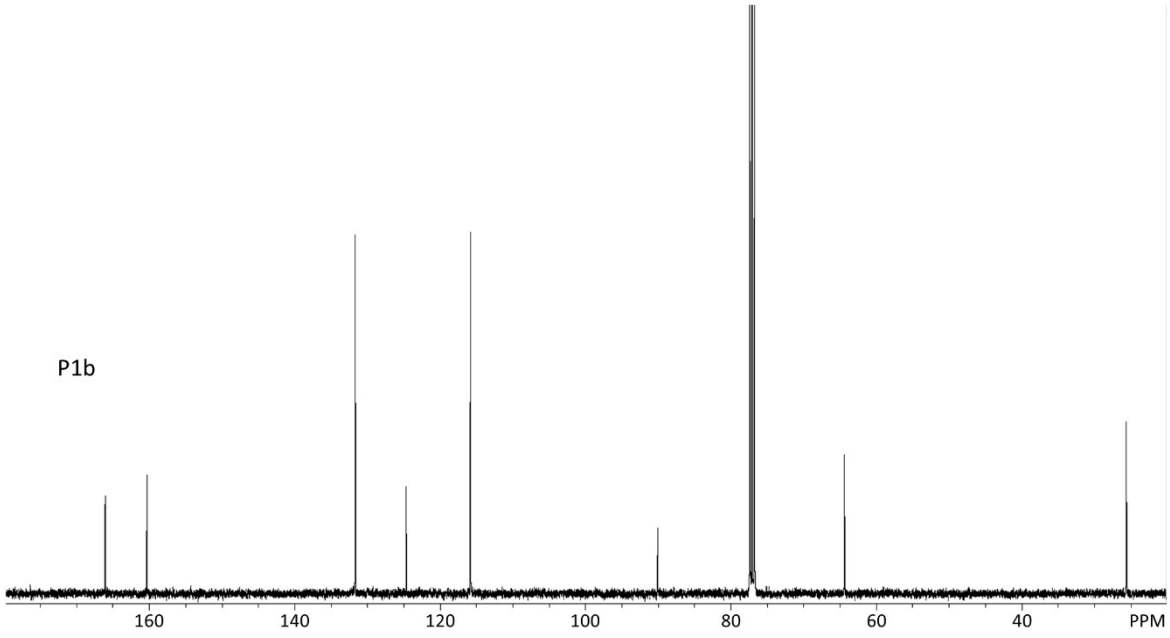

Figure S18. ^{13}C NMR spectrum of **P1b**.

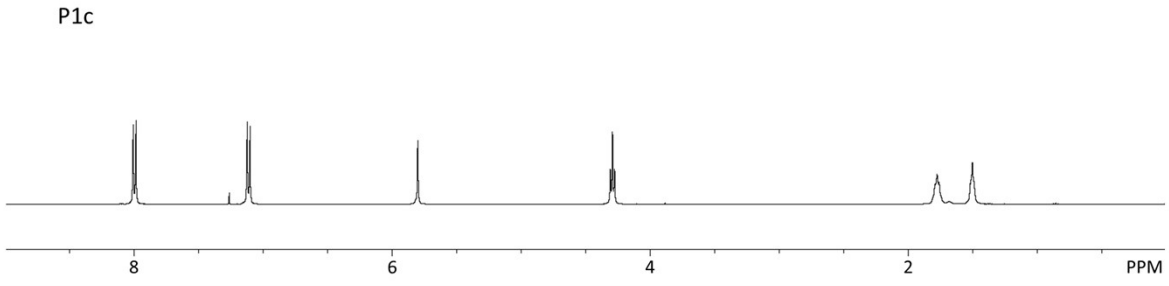

Figure S19. ^{1}H NMR spectrum of **P1c**.

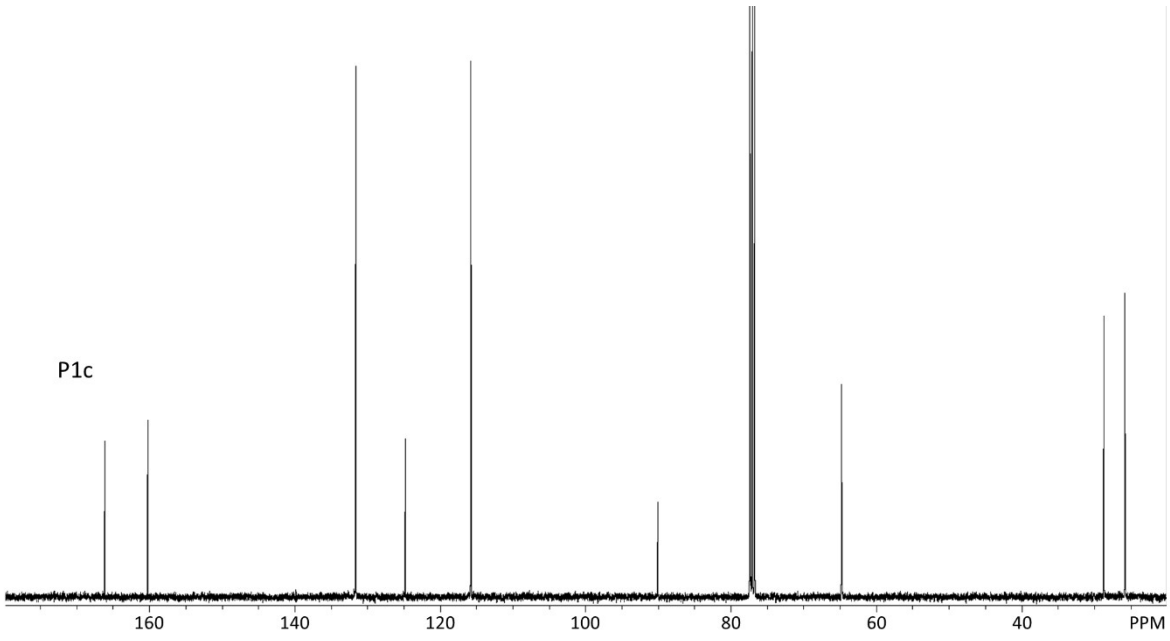

Figure S20. ^{13}C NMR spectrum of **P1c**.

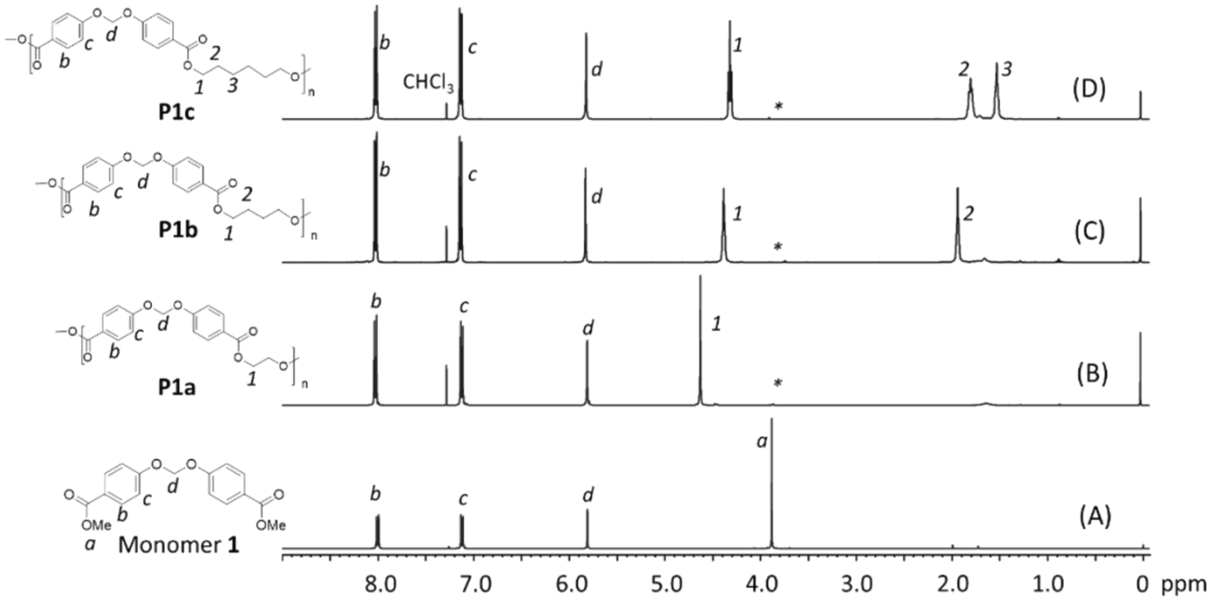

Figure 21. ^{1}H NMR spectra of Monomer 1 and polyesters P1a-c in $CDCl_3$.

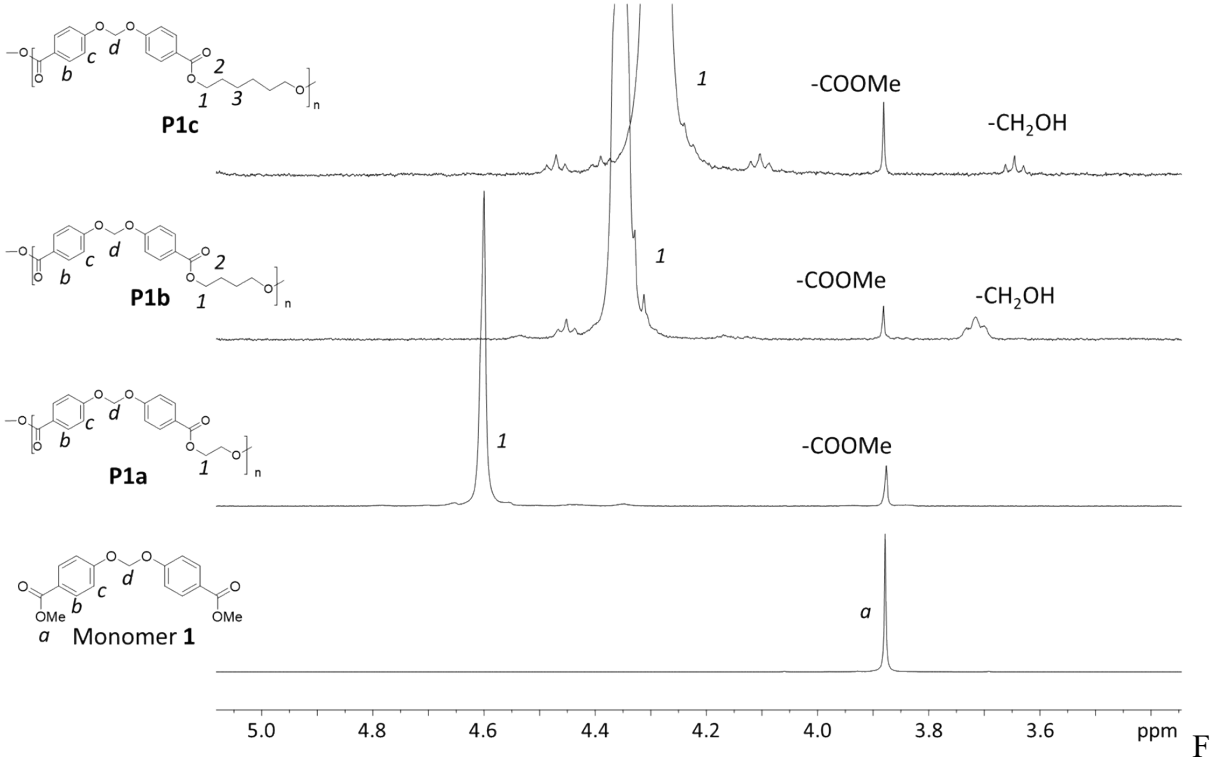

Figure S22. Zoomed-in ^{1}H NMR spectrum of Monomer **1** and polyesters **P1a-c** in $CDCl_3$.

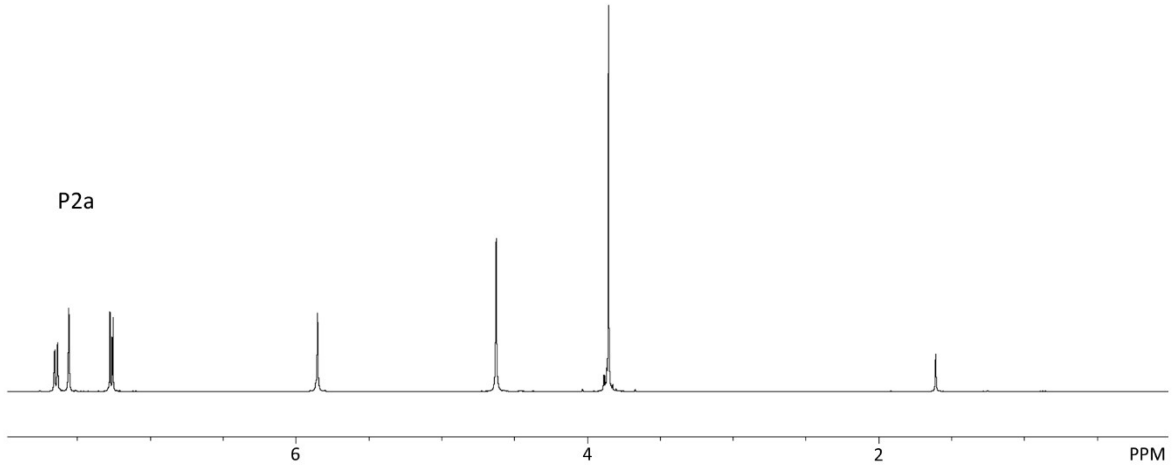

Figure S23. ^{1}H NMR spectrum of **P2a**.

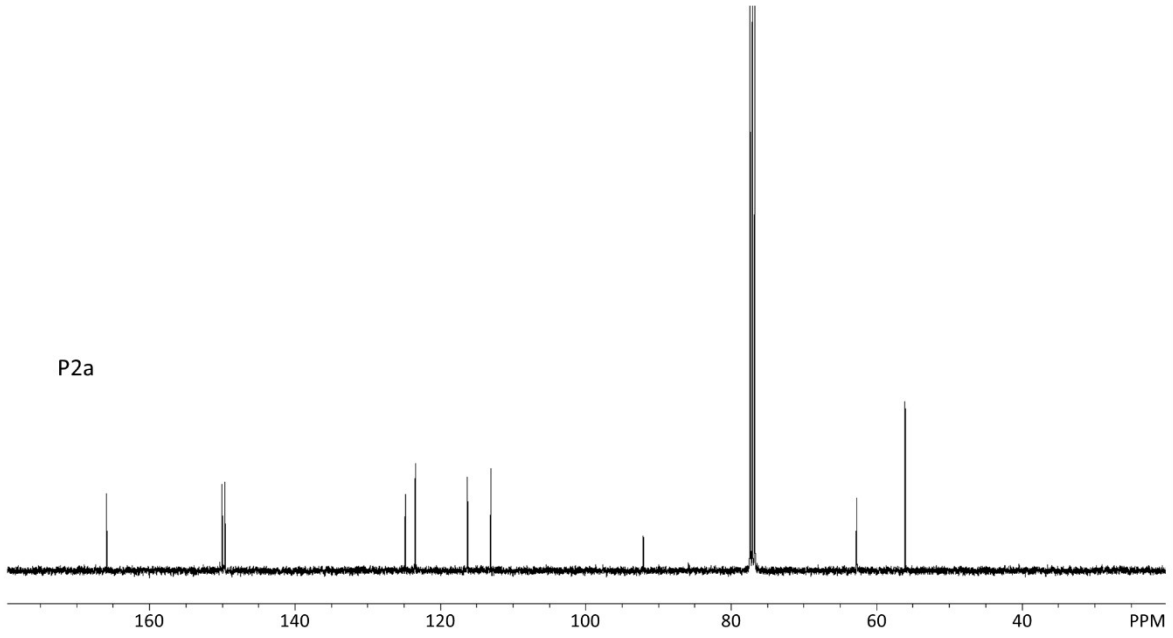

Figure S24. ^{13}C NMR spectrum of **P2a**.

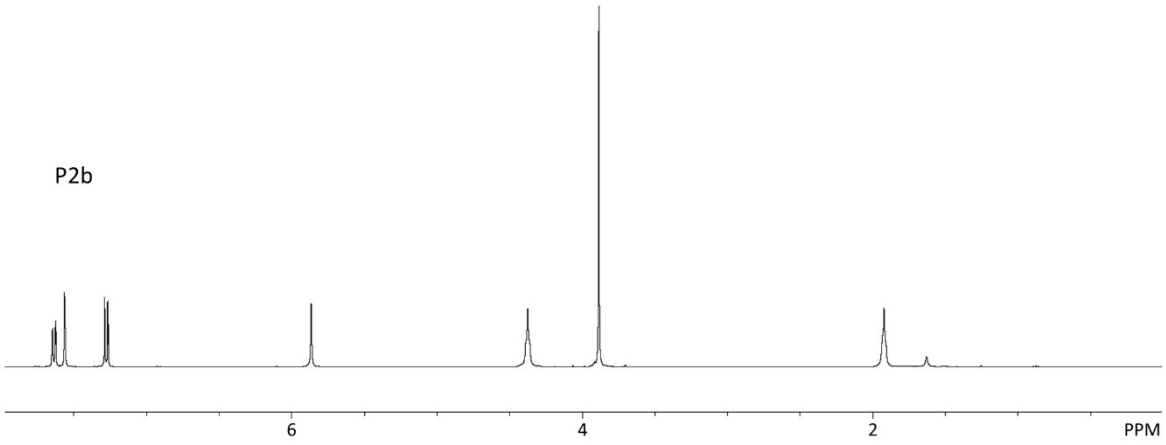

Figure S25. ^{1}H NMR spectrum of **P2b**.

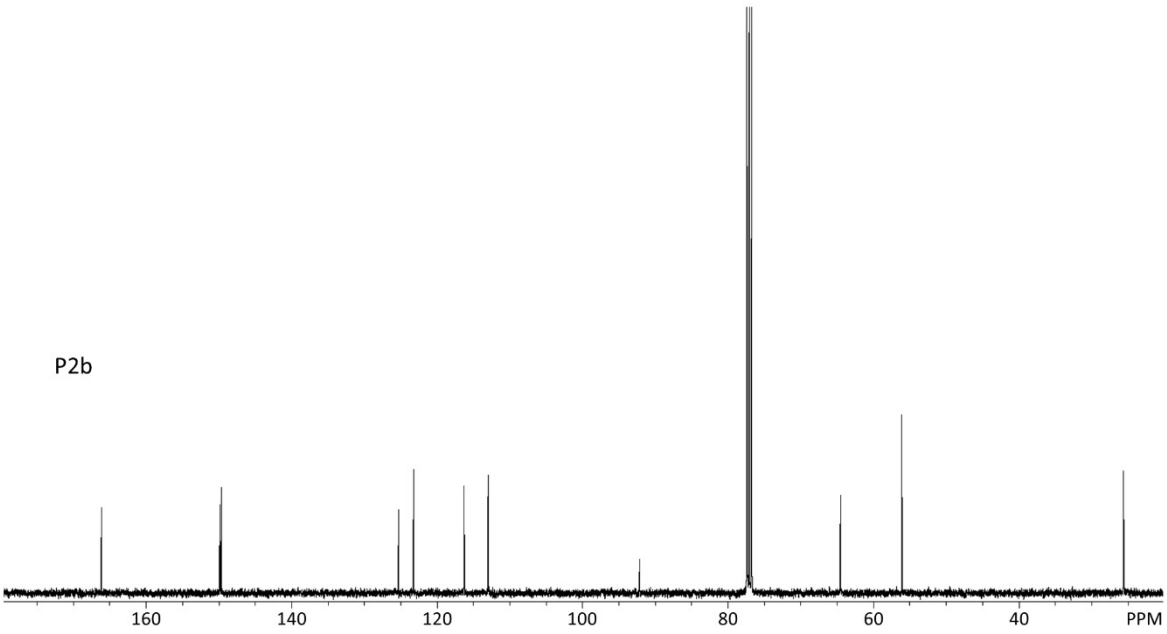

Figure S26. ^{13}C NMR spectrum of **P2b**.

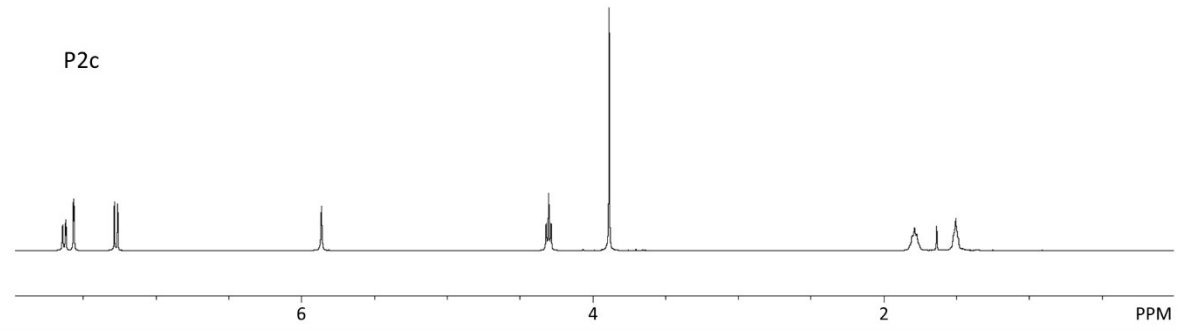

Figure S27. ^{1}H NMR spectrum of **P2c**.

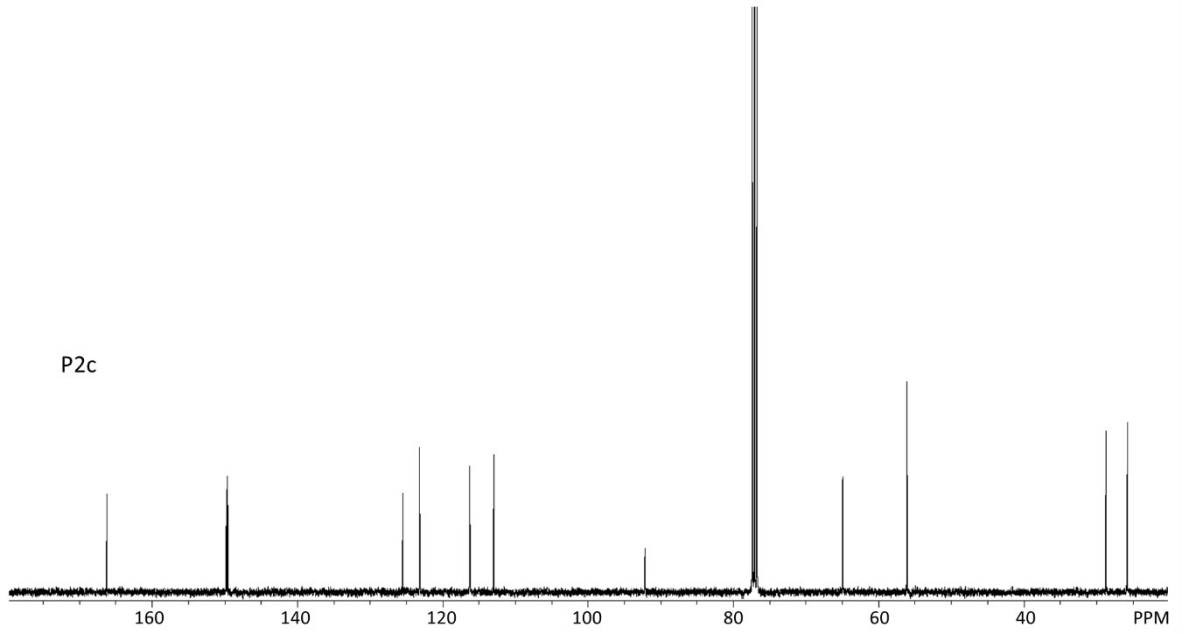

Figure S28. ^{13}C NMR spectrum of **P2c**.

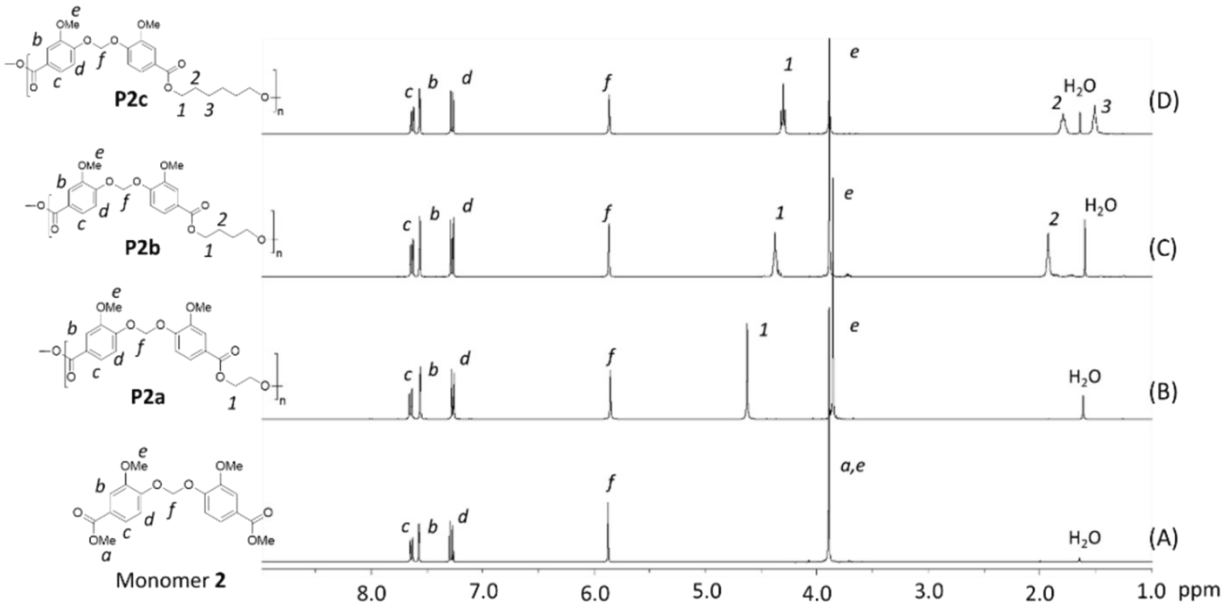

Figure S29. ^{1}H NMR spectra of Monomer 2 and polyesters P2a-c in $CDCl_3$.

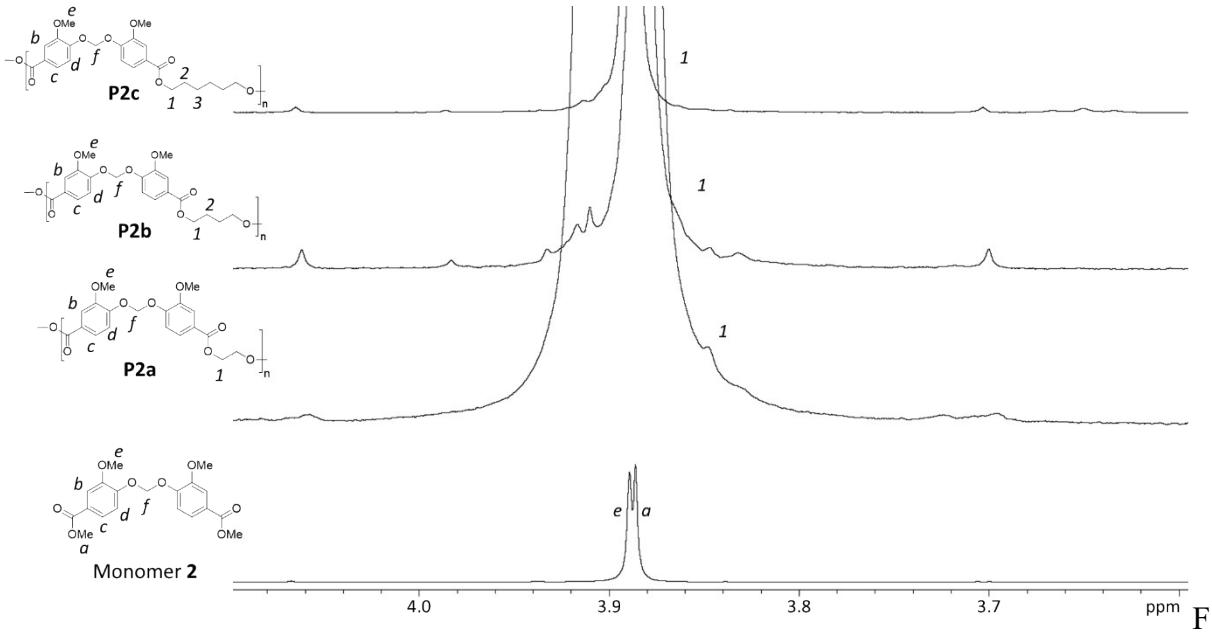

Figure S30. Zoomed-in ^{1}H NMR spectrum of monomer **2** and polyesters **P2a-c** in $CDCl_3$.

5. FTIR spectra for P1a-c and P2a-c

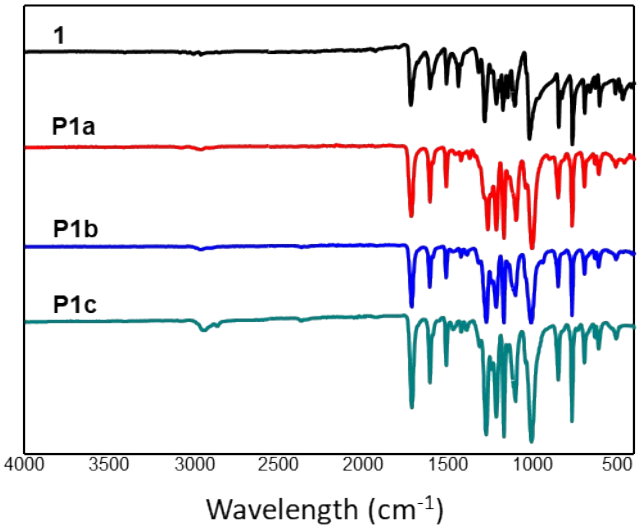

Figure S31. FTIR spectra of monomer **1** and polymers **P1a-c**.

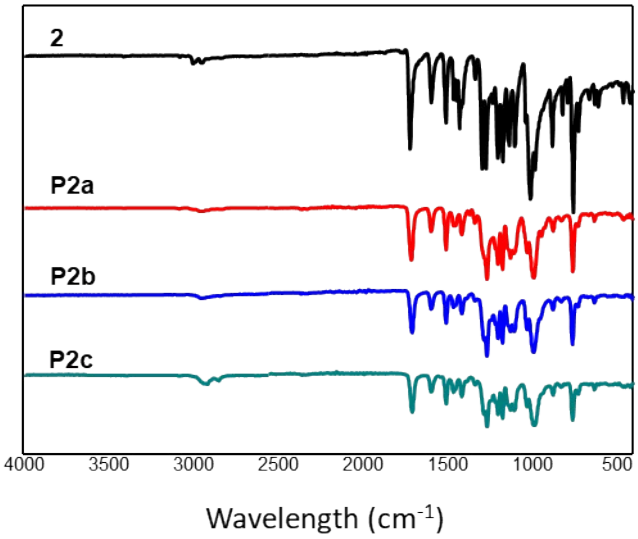

Figure S32. FTIR spectra of monomer **2** and polymers **P2a-c**.

6. Polymer hydrolysis studies

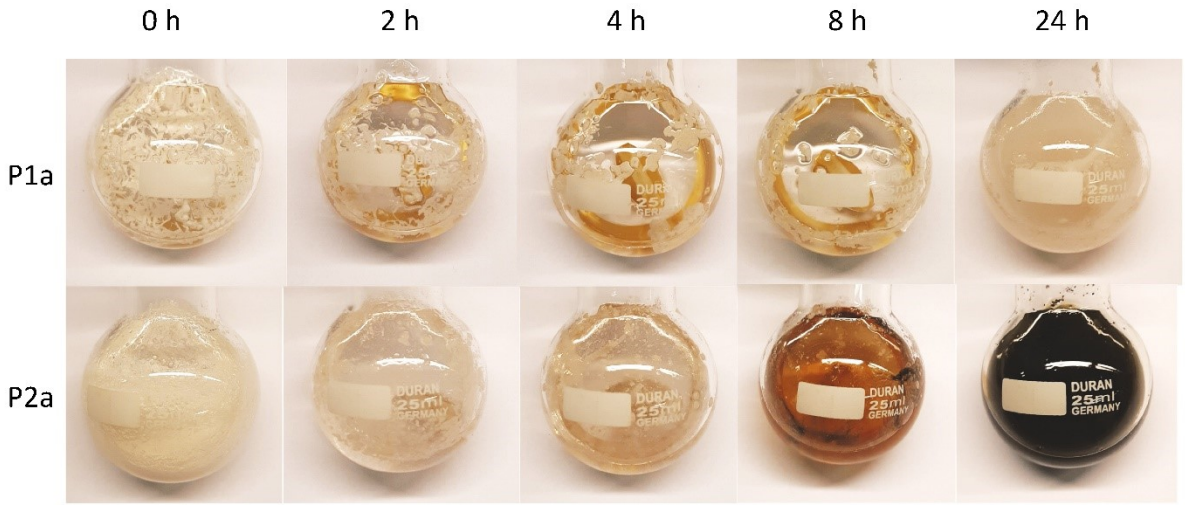

Figure S33. Photographs taken during the acidic hydrolysis of **P1a** and **P2a** in concentrated aqueous HCl (12 M).

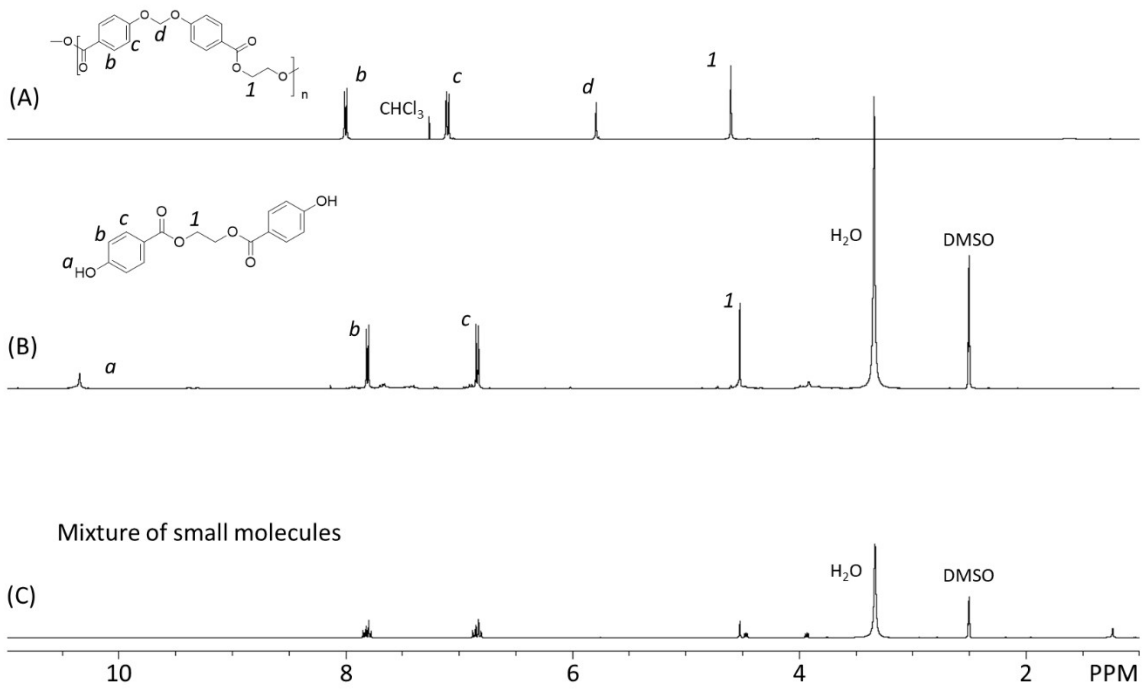

Figure S34. ^{1}H NMR spectra of (A) initial **P1a** in $CDCl_3$, (B) the solid collected after hydrolysis, and (C) the extracted organic phase.

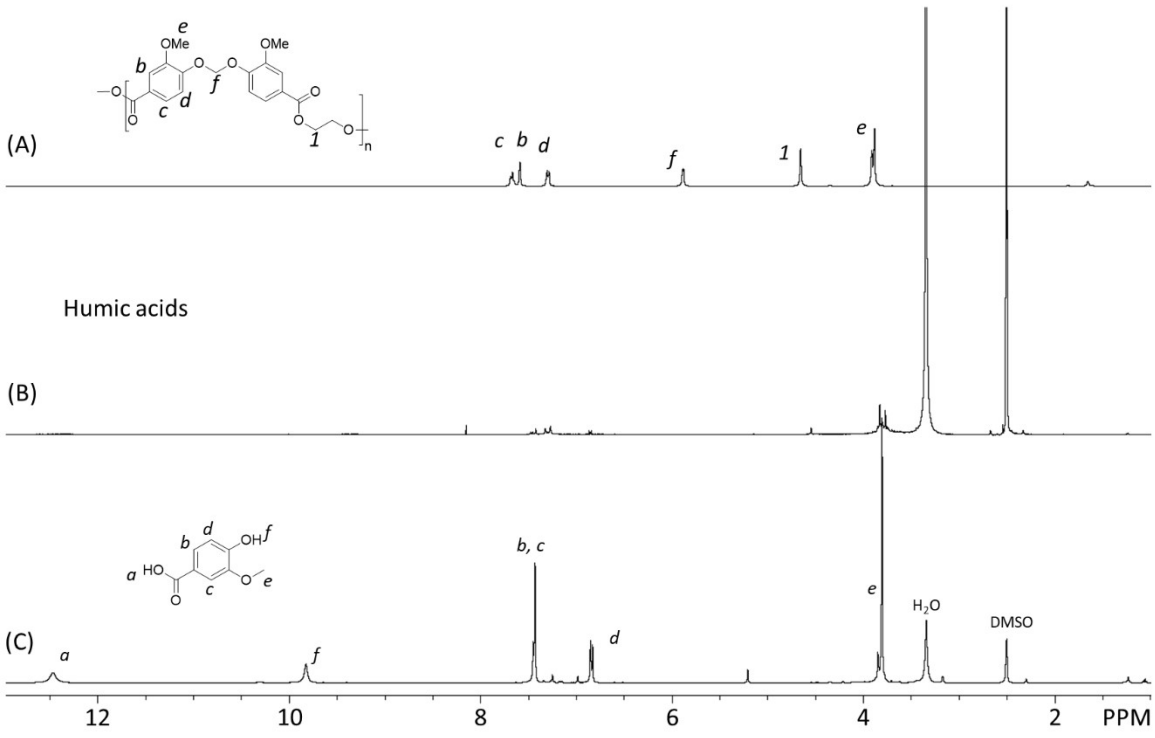

Figure S35. ^{1}H NMR spectra of (A) initial **P2a** in $CDCl_3$, (B) the solid collected after hydrolysis, and (C) the extracted organic phase.

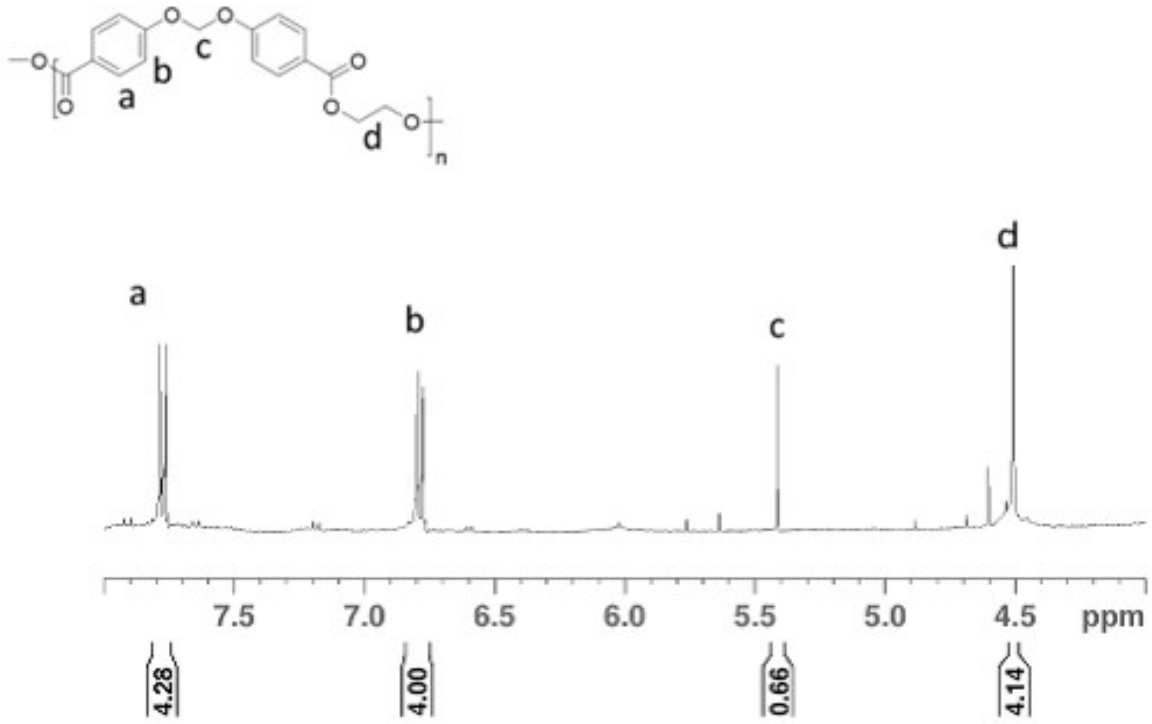

Figure S36. ^{1}H NMR spectrum of the crude product formed by direct repolymerization of **BP1** (recovered from hydrolyzed **P1a**) with dibromomethane.

Table S3. Hydrolysis of **P2a** under different HCl concentrations.

Reaction	C_{HCl} (M)	Solid Residue	Filtrate
A	3	92 %	2 %
B	6	89 %	3 %
C	9	72 %	13 %
D	10.5	45 %	15 %
E	12	21 %	31 %

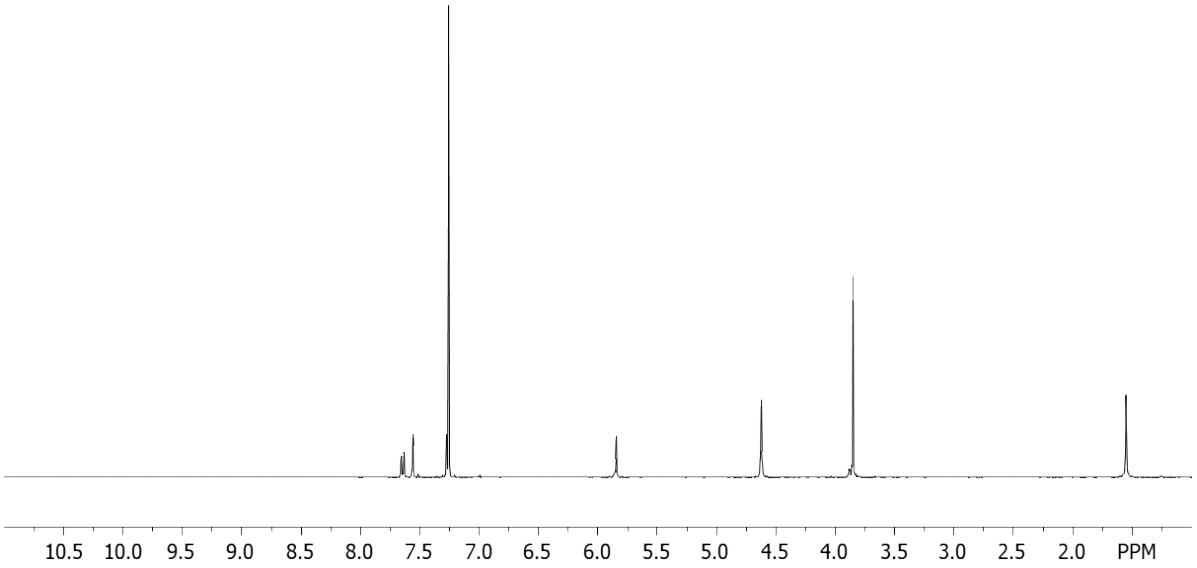

Figure S37. ^{1}H NMR spectrum of solid residue after hydrolysis of **P2a** in HCl (3M).

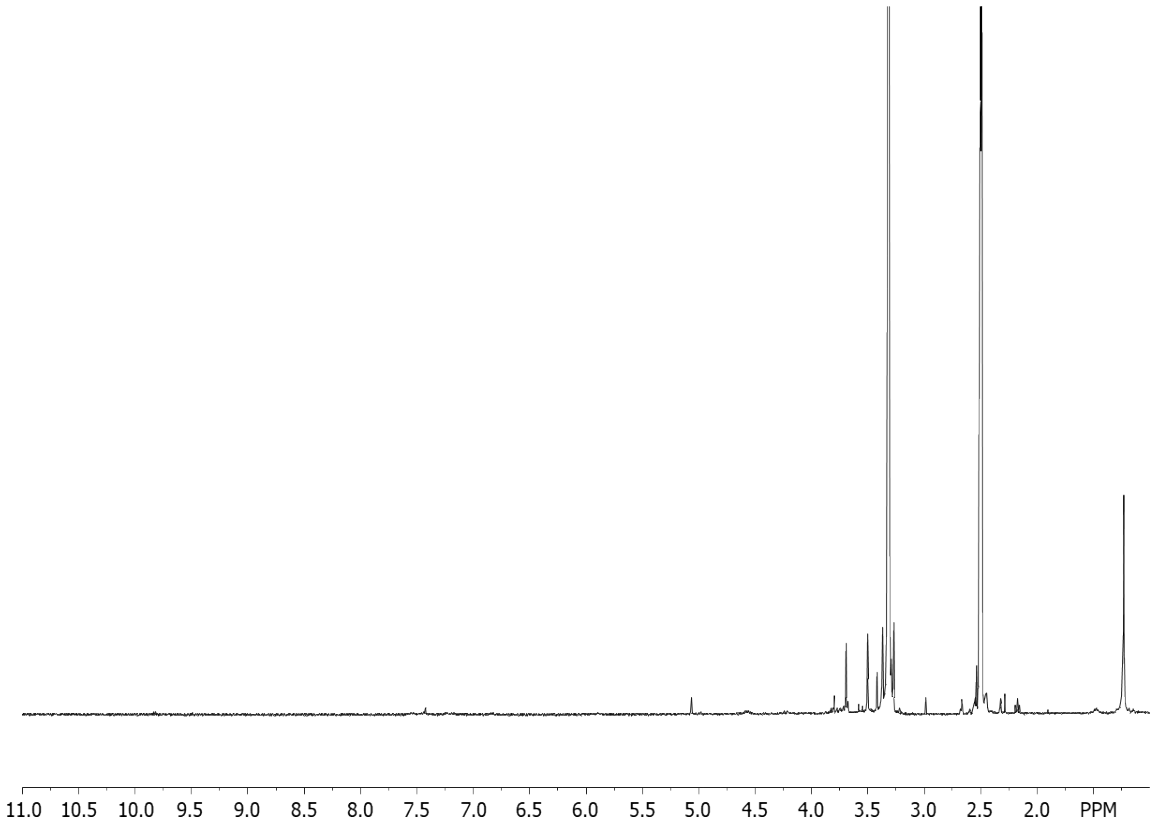

Figure S38. ^{1}H NMR spectrum of concentrated filtrate after hydrolysis of **P2a** in HCl (3M).

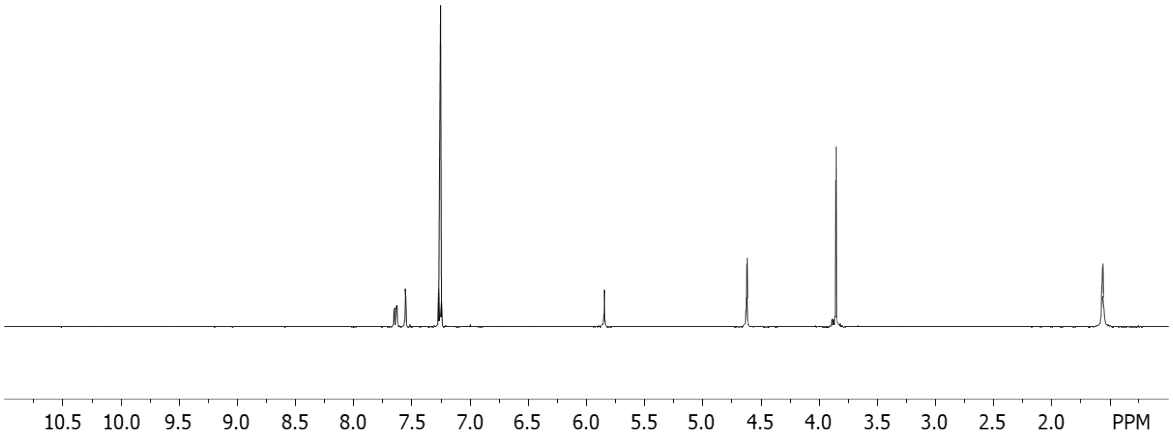

Figure S39. ^{1}H NMR spectrum of solid residue after hydrolysis of **P2a** in HCl (6 M).

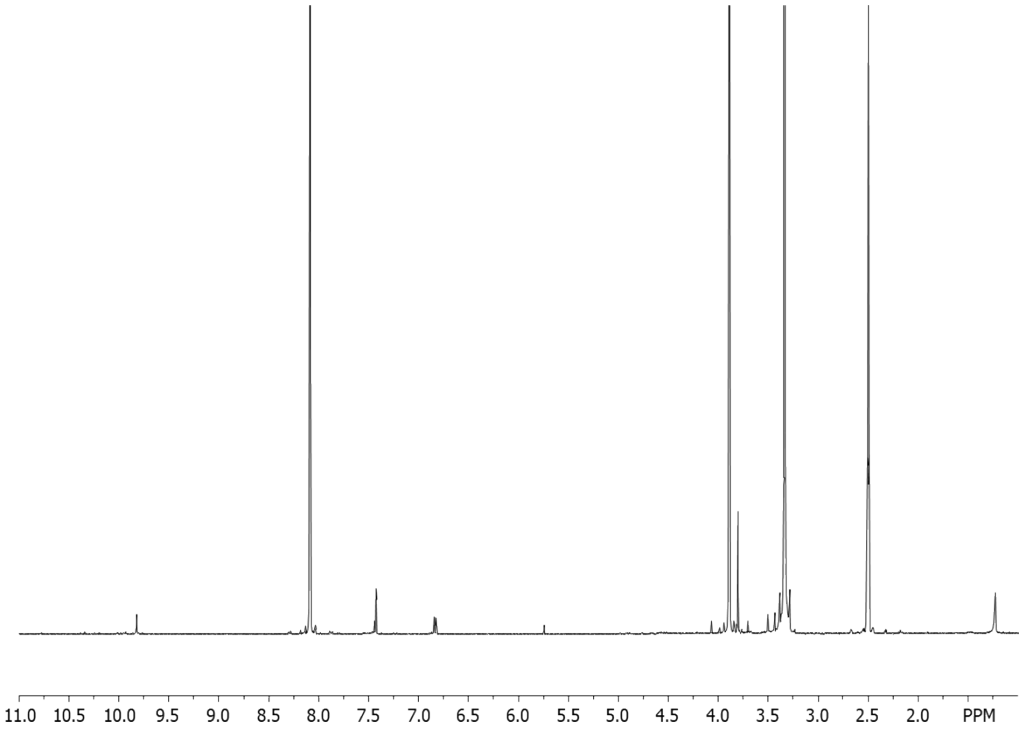

Figure S40. ^{1}H NMR spectrum of concentrated filtrate after hydrolysis of **P2a** in HCl (6 M).

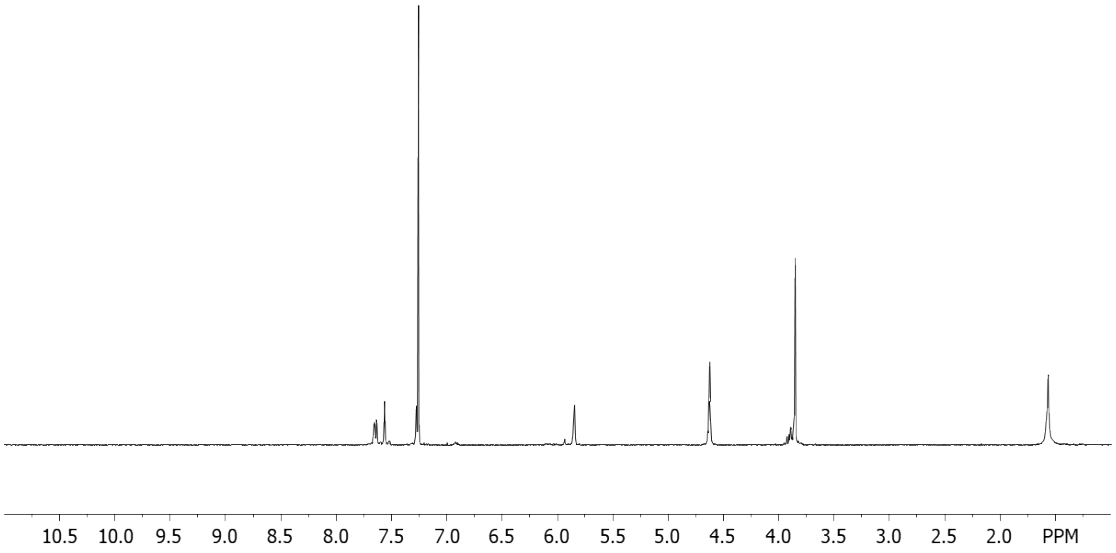

Figure S41. ^{1}H NMR spectrum of solid residue after hydrolysis of **P2a** in HCl (9 M).

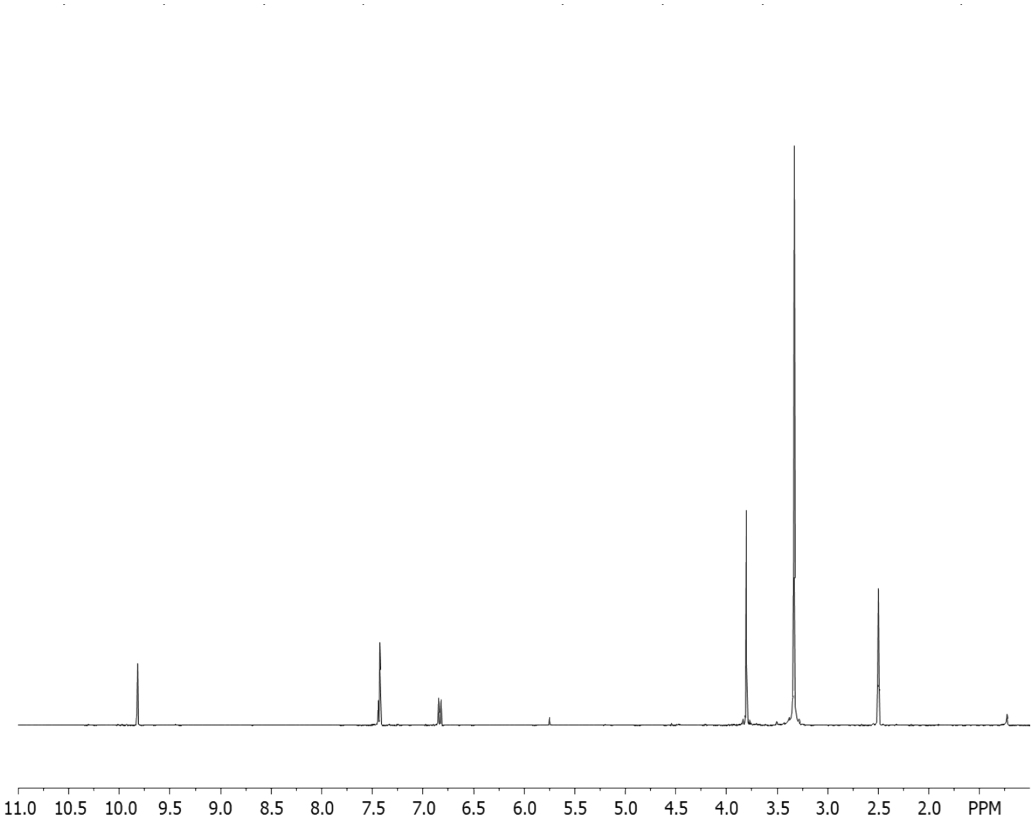

Figure S42. ^{1}H NMR spectrum of concentrated filtrate after hydrolysis of **P2a** in HCl (9 M).

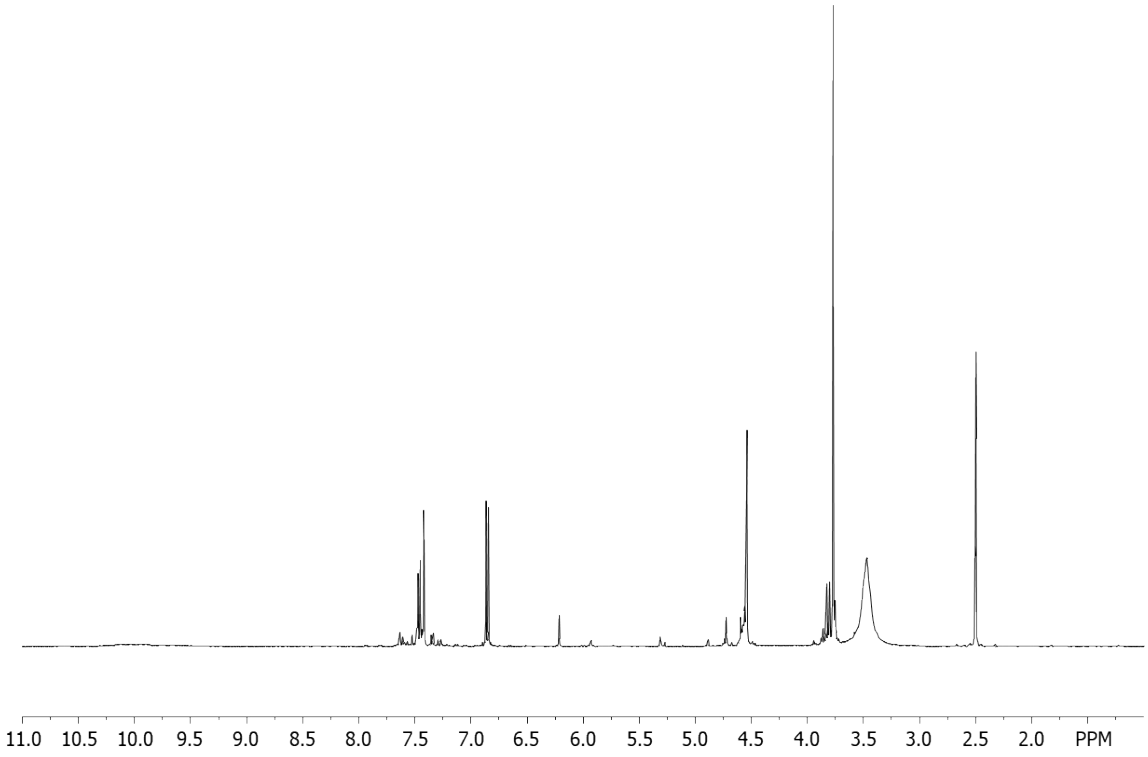

Figure S43. ^{1}H NMR spectrum of solid residue after hydrolysis of **P2a** in HCl (10.5 M).

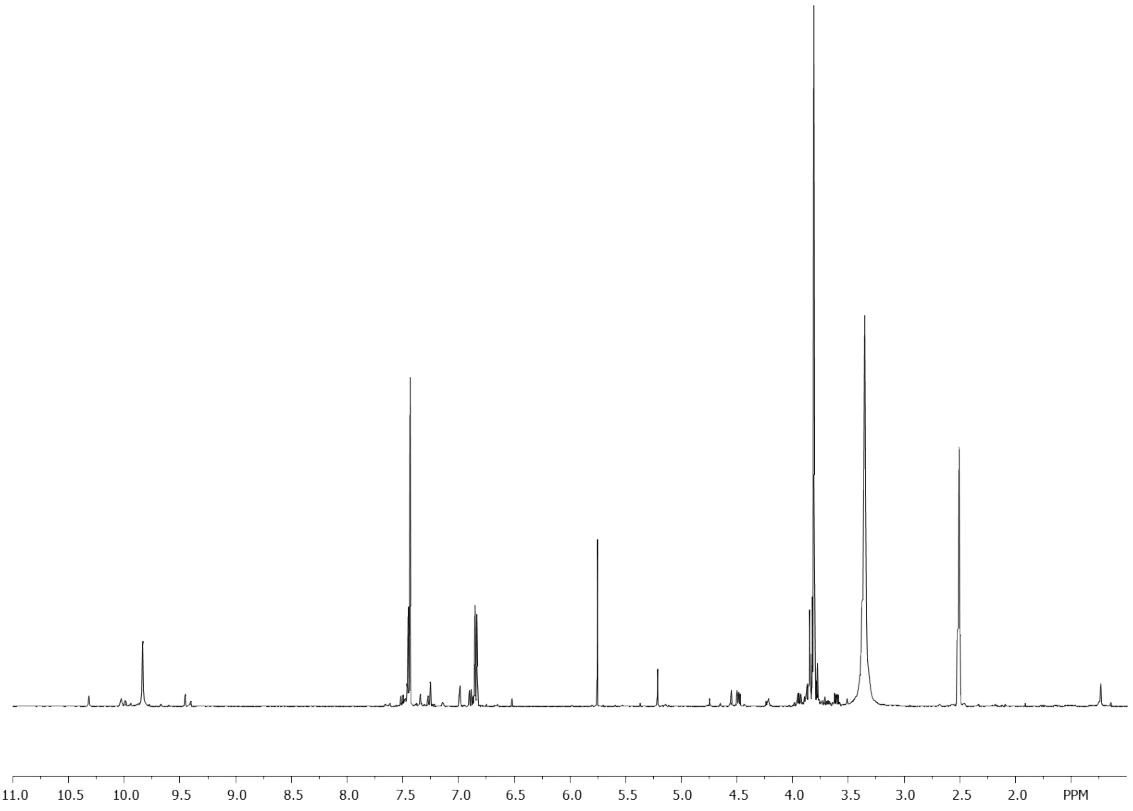

Figure S44. ^{1}H NMR spectrum of concentrated filtrate after hydrolysis of **P2a** in HCl (10.5 M).

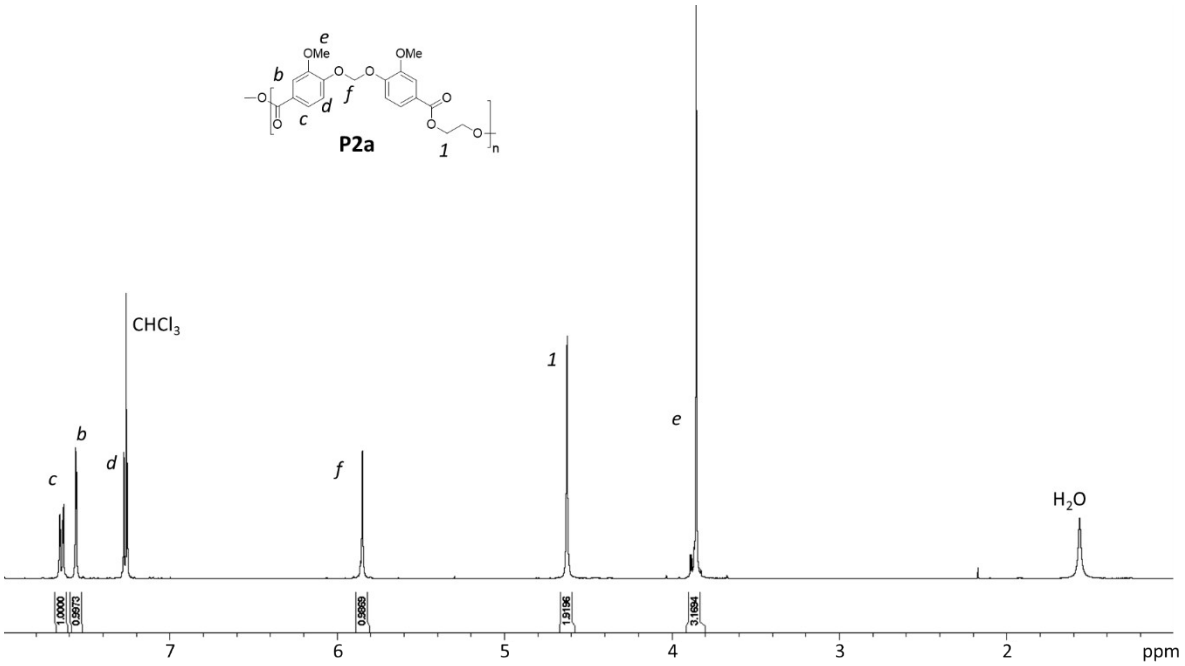

Figure S45. ^{1}H NMR spectrum of **P2a** after being stirred for 24 h in formic acid/H_2O (50/50) at 70 °C.

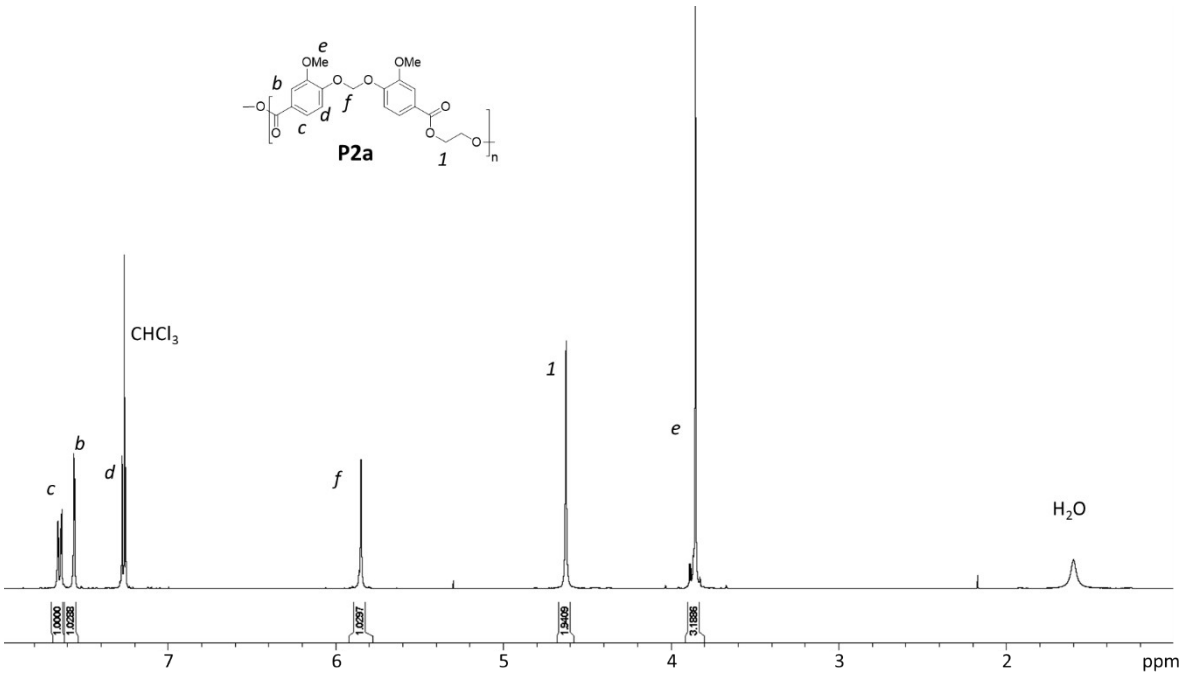

Figure S46. ^{1}H NMR spectrum of **P2a** after being stirred for 24 h in an oxalic acid solution (70 g/L) at 70 °C.

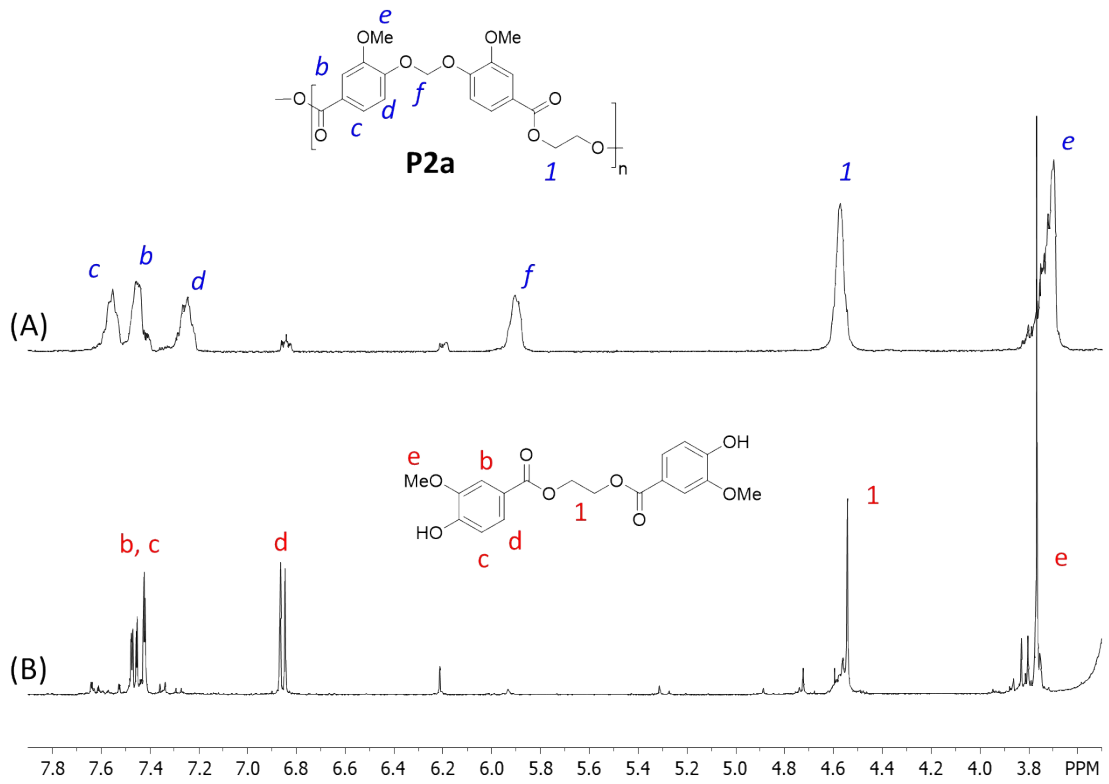

Figure S47. ^{1}H NMR spectra in DMSO-d_6 of the solid residues from **P2a** after hydrolysis for 24 h in 9M HCl (A) and 10.5 M HCl (B).

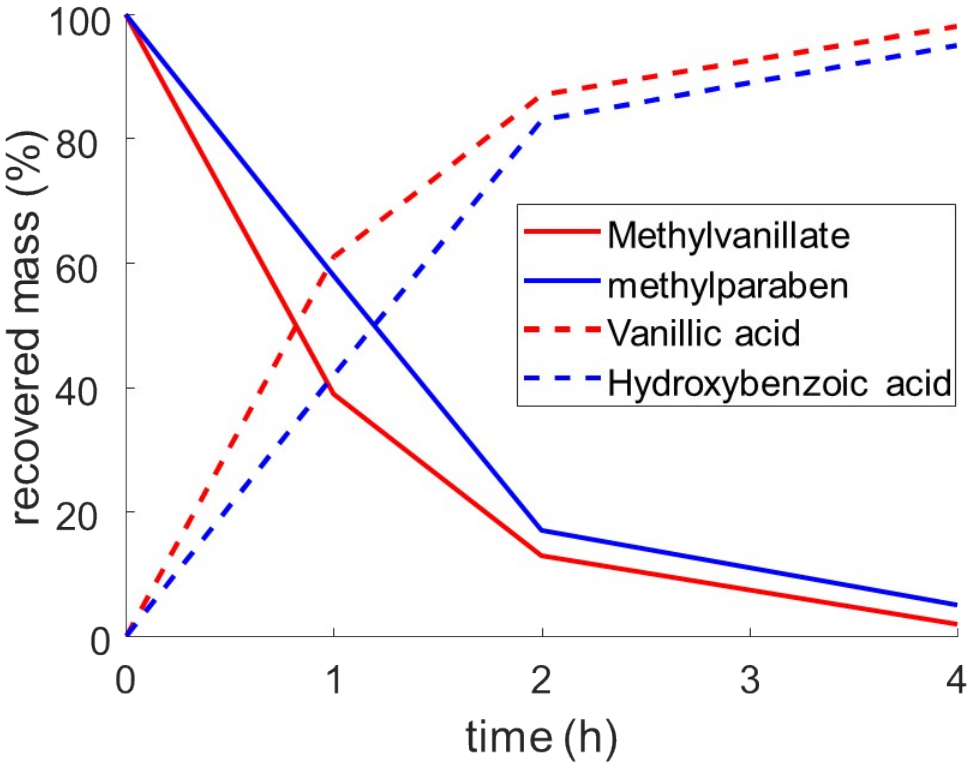

Figure S48. Kinetics of the acidic hydrolysis of methyl vanillate and methyl paraben to vanillic acid and hydroxybenzoic acid, respectively, in concentrated aqueous HCl (12 M).

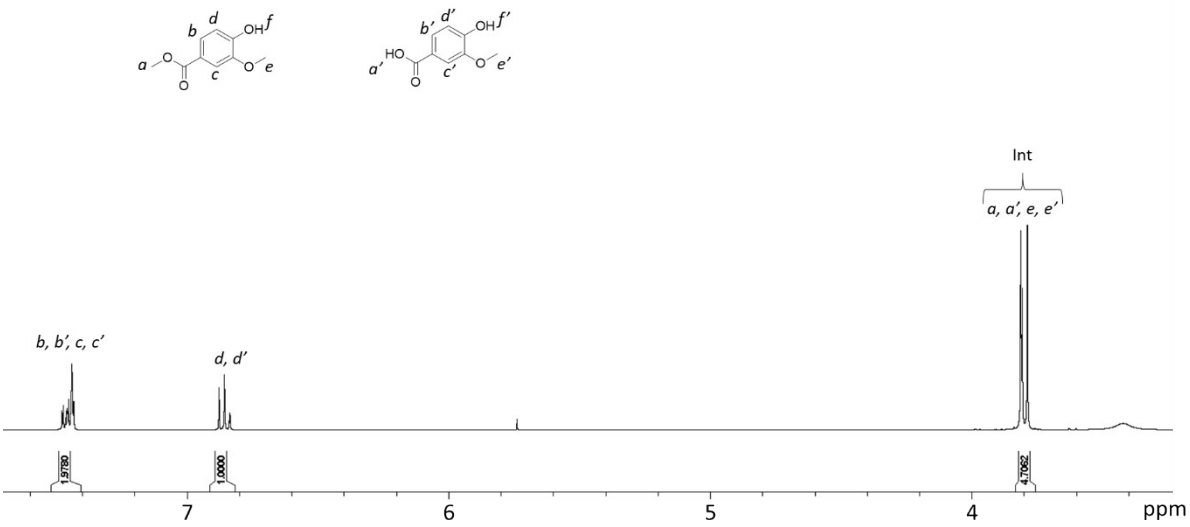

Figure S49. [1]H-NMR spectrum of the solid recovered by filtration after acidic hydrolysis of methylvanillate.

The content of methyl vanillate and vanillic acid in the sample collected by filtration and the sample collected by solvent extraction was calculated according to the following equations:

Eq. 2
$$Int = 6 * X_{n\_vanillate} + 3 * (1 - X_{n\_vanillate})$$

Eq. 3
$$X_{m-vanillate} = \frac{X_{n-vanillate} * M_{methylvanillate}}{(X_{n-vanillate} * M_{methylvanillate} + X_{n-acid} * M_{vanillic\ acid})}$$

Eq. 4
$$m_{vanillate} = X_{m-vanillate} * m_{sample}$$

We assume that the difference between the starting mass and the collected mass was caused by the polar vanillic acid partially remaining in the aqueous phase. The remaining fraction of methylvanillate in the reaction was calculated.

Eq. 5
$$X_{m-vanillate-tot} = \frac{m_{vanillate-filt} + m_{vanillate-extr}}{m_0}$$

Int = integral of both methoxy groups compared to the aromatic proton *d* (see Fig. S29).

$X_{m\text{-}vanillate}$ = mass fraction of methyl vanillate in the sample.

$X_{n\_vanillate}$ = molar fraction of methyl vanillate in the sample.

X_{n_acid} = molar fraction of vanillic acid in the sample.

$M_{methylvanillate}$ = 182.17 g/mol

$M_{vanillic\ acid}$ = 168.15 g/mol

m_{sample} = total mass in sample.

$m_{vanillate}$ = total mass of ester in sample.

m_0 = total mass at the start of the reaction.

$m_{vanillate\text{-}filt}$ = total mass methylvanillate in the solid collected by filtration

$m_{vanillate\text{-}extr}$ = total mass methylvanillate in the solid collected by solvent extraction

$X_{m\text{-}vanillate\text{-}tot}$ = mass fraction methylvanillate in the reaction.

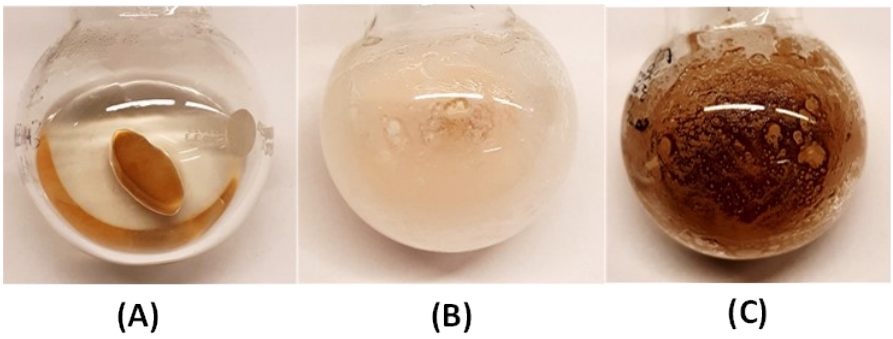

Figure S50. Methyl vanillate in HCl (12M) at 70 °C after 30 min (A), After 24 h (B), and after 2 h when a droplet of formaldehyde was added to the solution (C).

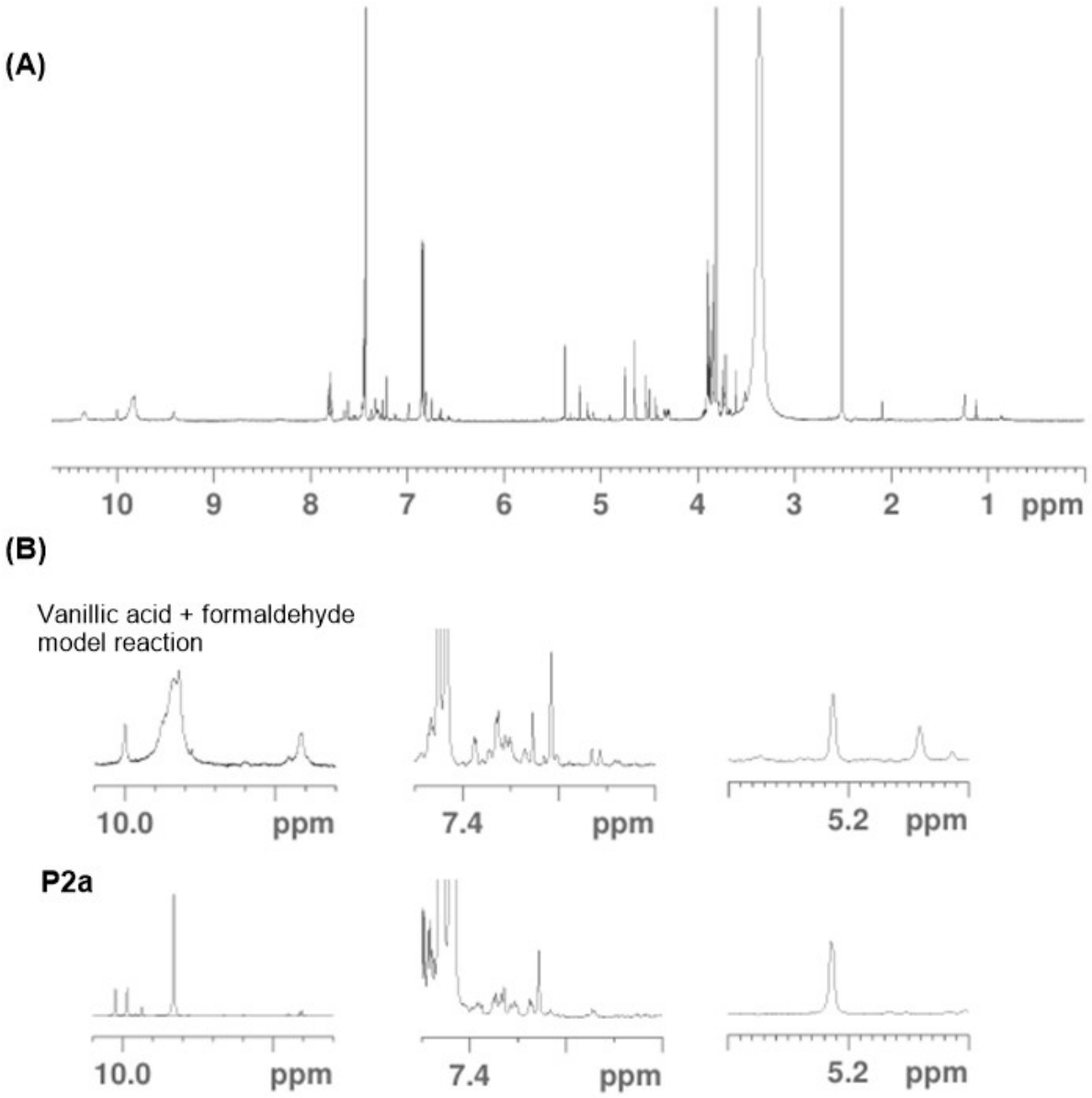

Figure S51. (A) ^{1}H NMR spectrum of concentrated filtrate obtained from the reaction between vanillic acid and formaldehyde in HCl 12 M at 70 °C for 2 h. (B) Comparison between ^{1}H NMR spectra of concentrated filtrate obtained from the vanillic acid + formaldehyde reaction and P2a hydrolysis in HCl 12 M at 70 °C for 2 h.

References

1 I. S. Modahl and E. Soldal, *The 2019 LCA of products from Borregaard , Sarpsborg*, 2019.

2 J. O. Krömer, R. G. Ferreira, D. Petrides and N. Kohlheb, *Front Bioeng Biotechnol*, 2020, **8**, 403.

3 J. Clayden, N. Geeves and S. Warren, *Organic Chemistry*, 2012.